DRFC-SCP

EUR-CEA-FC-1306

ACCURATE FREQUENCY MEASUREMENTS ON GYROTRONS USING A "GYRO-RADIOMETER"

L. Rebuffi

August 1986

ASSOCIATION EURATOM-CEA
DEPARTEMENT DE RECHERCHES
SUR LA FUSION CONTROLEE
CEN CADARACHE
[illegible] SAINT-PAUL-LEZ-DURANCE (FRANCE)

ACCURATE FREQUENCY MEASUREMENTS ON GYROTRONS USING A "GYRO-RADIOMETER"

L. Rebuffi

ACCURATE FREQUENCY MEASUREMENTS ON GYROTRONS USING A "GYRO-RADIOMETER"

L.Rebuffi

ASSOCIATION EURATOM-CEA SUR LA FUSION
Département de Recherches sur la Fusion Contrôlée
Centre d'Etudes Nucléaires
Boite Postale n°6. 92260 FONTENAY-AUX-ROSES (FRANCE)

Abstract

Using an heterodyne system, called "Gyro-radiometer", accurated frequency measurements have been carried out on VARIAN 60 GHz gyrotrons.

Changing the principal tuning parameters of a gyrotron, we have detected frequency variations up to 100 MHz, ~ 40 MHz frequency jumps and smaller jumps (~ 10 MHz) when mismatches in the transmission line were present.

FWHM bandwidth of 300 KHz, parasitic frequencies and frequency drift during 100 msec pulses have also been observed.

An efficient method to find a stable-, high power-, long pulse-working point of a gyrotron loaded by a transmission line, has been derived. In general, for any power value it is possible to find stable working conditions tuning the principal parameters of the tube in correspondance of a maximum of the emitted frequency.

INTRODUCTION

The Gyrotron, a high power millimeter wave source, based on stimulated cyclotron emission, has been developed in the last twenty years.
It consists (schemes in fig. 1 a,b) of an electron gun of the magnetron type which produces an annular electron beam. These electrons after being accelerated in a growing magnetic field, flow in a circular waveguide cavity (of dimension close to the cut-off for a TE_{0n} mode) where they interact with a R.F. wave. A relativistic phase bunching of the electrons (in presence of a static uniform magnetic field due to superconducting magnets) permits to transfer the electron azimuthal energy to the e.m. wave. Later on, the electron beam reaches the collector, and the high power wave exit through a vacuum window.
It is well known from gyrotron theory [1],[2],[3],[4], that the strongest generation of e.m. oscillation takes place when the frequency of one of the high-Q TE modes of the cavity is close to the fundamental electron resonance frequency Ω_c, following the fundamental equation :

$$\Omega - \Omega_c = k_{\parallel} \cdot v_{\parallel}$$

where Ω is the radiated frequency, $k_{\parallel} = \pi/L$ depends on the cavity length L, $v_{\parallel}$ is the electron velocity parallel to the cavity axis and

$$\Omega_c = (e.B) / (\gamma.m_0)$$

e and m_0 are the charge and the rest mass of an electron, $\gamma=1+(Vc/511)$ is the relativistic factor, Vc is the Cathode Voltage in KV.
An almost linear frequency increase with the magnetic field has been experimentally shown (about 200 MHz/KG) [5]. The "S" shape line of the frequency f versus the cavity magnetic field , should be explainable using a non linear theory [6].
Frequency tuning of a gyrotron of the order of 100 MHz or more, has been verified too [5],[6].
A frequency decrease has been obtained increasing the Cathode Voltage Vc [6]. Besides it is known that an increase of frequency corresponds to a power decrease [7] and that there is a certain distance between

the frequencies of the possible resonating modes in the cavity [5],[7]. Anomalous frequency behaviours are reported in [6],[8] showing frequency jumps and "U" shape for the frequency variation. Nevertheless a really detailed frequency measurement of a gyrotron had never been performed.

Accurate frequency measurements are necessary not only for developers but also for gyrotron users. In fact, a frequency control permits a correct use of the source, avoiding spurious modes oscillations at wrong frequencies (thus avoiding localized heating due to trapped modes between the gyrotron window and the cavity). Moreover when a power transmission line is connected with a gyrotron, mismatches could be present. Spurious modes generated by the source or by the line could cause either high losses or breakdowns due to trapped modes in the line, or power reflection. These problems became more and more important for long pulses or CW regimes. Besides a bad VSWR can reduce the output power up to 30% [5]. Therefore, as the frequency behaviour of a gyrotron is sensitive to a mismatch in the line, an accurate frequency measurement could bring informations about the gyrotron/line matching.

For these reasons we have decided to control carefully the signals emitted from the three 60 GHz -200 KW 100 msec pulsed gyrotrons (VARIAN VGE 8060 B SN 011/012/013 with complex cavity TE_{011} - TE_{021}) used for the ECRH experiment in the TFR tokamak. Frequency variations of each gyrotron have been measured for variations of the most significant tuning parameters of the source. The parameters variation range was limited to a safety working zone, indicated by the constructor. The measurements have been effectued using a radiometer to detect the signal coming out of the gyrotrons.

The heterodyne system permitted to detect on a single shot real-time base even weak or parasitic modes in presence of a strong principal mode signal.

The precision of the measurements, the interesting frequency behaviour of the gyrotrons, the possibility to tune a gyrotron using this frequency measurement, and the fiability of the device, pushed us to call this instrument : "Gyro-Radiometer".

1 THE GYRO-RADIOMETER

A high power millimiter wave is emitted by the gyrotron in an oversized circular waveguide (ϕ = 63.5 mm). The first component of the transmission line, an arc detector, couples this wave into a standard rectangular waveguide, by mean of a non calibrated hole (coupling coefficient in the 50-60 dB range). Then the signal enters the gyro-radiometer as shown in fig. 2. The lack of a mode-selective coupling does not permit a power calibration at the detection. This wave is then coupled with a signal from a local oscillator (L.O.). We have used a VARIAN klystron (VRE 2103 A-73 Power ~ 500-1000 mW) tunable in frequency (56.9-62.9 GHz), but cheaper and simpler centimetric source to handle, as a Gunn diode, can be used as well in one of its harmonics. A cavity wavemeter (THOMSON-CSF) gives an absolute frequency measurement of the sources, with an absolute error of about $\pm$ 60 GHz and an instrumental resolution of 10 MHz. Variable attenuators are used to modulate the amplitude of the signals. At the end of the device a wide-band detector can be used to detect the beating wave. Otherwise, if a centimetric L.O. is used, the gyrotron signal can beat directly in an harmonic mixer. The signal is then sent to a spectrum analyser (we used a H.P. 8552 B IF section, 8553 B RF section). A 300 KHz filter and a scanning time varying between 0.2 msec and 1 msec has been used. A large frequency scan ($\pm$3 GHz) is possible varying the frequency of the klystron, while the spectrum analyser permits a precise scan (in our experiment reduced at the 0-110 Mhz range).

With this system it is also possible to detect the beating of the signals emitted by two gyrotrons, when the local source is excluded. This experience has been successfully carried out, using the Gyrotrons # 011 and # 012. Changing their tuning parameters, we have obtained a beating frequency in the range 10-80 MHz ($\omega_{011} - \omega_{012}$) detected by the Gyro-radiometer. The total output power was always greater than 350 KW. The plasma in the tokamak, considered as a nonlinear medium, was probably sensible to this beating, but the coupled power was very low to detect a visible effect of resonance on the ionic population.

2 THE BEATING EQUATION

The signal emitted by the gyrotron at a frequency ω_1 can be described by the expression

$$E_1 = A_1 \cos(\omega_1 t + \varphi_1)$$

This wave will enter the gyro-radiometer and beat with the wave generated by the L.O. at a frequency ω_2 (close to ω_1) which can be described by

$$E_2 = A_2 \cos(\omega_2 t + \varphi_2)$$

The beating intensity of the two signals detected by the mixer is:

$$I \sim (E_1 + E_2)^2 \rightarrow$$

$$I \sim (A_1)^2/2 + (A_2)^2/2 + \quad \text{(constant terms)}$$

$$+ (A_1)^2/2 \cos(2\omega_1 t+2\varphi_1) + (A_2)^2/2 \cos(2\omega_2 t+2\varphi_2) +$$

$$+ A_1 A_2 \cos[(\omega_1+\omega_2)t + (\varphi_1+\varphi_2)] + \quad \text{(high frequency terms)}$$

$$+ A_1 A_2 \cos[(\omega_1-\omega_2)t + (\varphi_1-\varphi_2)] \quad \text{(low frequency term)}$$

If two frequencies ω_1 and ω_2 are present, only the low frequency term will be detected by the mixer. Thus, on the spectrum analyser we will see the difference of the two frequencies (in our experiment we always kept the position: ω gyrotron $< \omega$ local source).
If spurious frequencies appear, the analysis becames more complicate. Supposing to have a spurious frequency ω_3 with

$$E_3 = A_3 \cos(\omega_3 t + \varphi_3)$$

then the intensity of the low frequency detected signal will be:

$$I = A_1A_2 \cos[(\omega_1 - \omega_2)t + (\varphi_1 - \varphi_2)] +$$

$$+ A_1A_3 \cos[(\omega_1 - \omega_3)t + (\varphi_1 - \varphi_3)] +$$

$$+ A_2A_3 \cos[(\omega_2 - \omega_3)t + (\varphi_2 - \varphi_3)]$$

To avoid three spectral lines, it is better to take $A_2 \gg A_1$ and $A_2 \gg A_3$, controlling A_2 with the attenuator. In this case there will be only the principal spike $(\omega_2 - \omega_1)$ and the spurious one $(\omega_2 - \omega_3)$. Moreover, beating harmonics of the type $n.(\omega_2 - \omega_1)$, have to be avoided. Anyway they are easy to recognize, and a small variation in the reference frequency of the L.O. is sufficient to move them out of the detection range.

3 GENERALITIES ON THE FREQUENCY MEASUREMENTS

The local low power source used was a klystron delivering a stable reference signal (frequency fluctuations less than 250 KHz during a 100 msec gyrotron pulse). In the spectrum analyser, a 300 KHz filter has been used. Thus the precision in the frequency measurement is 3.10^5 Hz / 60.10^9 Hz ≈ 5.10^{-6} .

All parasitic signals leading to spurious spectral lines can be easily avoided with a careful mounting.

During a pulse the used spectrum analyser scans only once the frequency range in the preset time. We usually detected the spectral line in the middle of a pulse. When necessary, we have moved the scanning time all along the pulselength.

Even if the absolute frequency measurement given by a cavity wavemeter had an incertitude of ± 60 MHz, the relative frequency measurement assured by the heterodyne system permitted at least, a precision in the order of few hundreds KHz. The reproductibility of the frequency measurement and of the gyrotron setting was limited only by instrumental precision and by stability (which nevertheless was rather good) of the electrical setting parameters of the tube.

Within these limits this heterodyne system gave a precise frequency measurement and an easy and good reproductibility of the measures.

In the frequency measurements carried out for each gyrotron, parameter variation curves have been obtained changing only one parameter at a time while others were kept constant.

Pulses of 10 msec have been used, with a scan time of 1 msec. The variation range for each parameter was in the safe working zone (given by the constructor), to avoid dangerous or anomalous regimes. This has limited the variation of the gyrotron parameters in the ranges reported in table I.

The set up for the frequency measurement at the gyrotron exit, using an arc detector and a water load, is shown in fig. 3 . Sometimes frequency tests have been performed connecting a gyrotron with part of a transmission line. In this case the used scheme is shown in fig. 4.

Beam Current	I_B	5 or 8 Amps
Cathode Voltage	V_C	-80 KV ± const.
Top Main Coil Current	I_1	17.70-18.70 Amps
Bottom Main Coil Current	I_2	14.00-14.30 Amps
Cathode Coil Current	I_S	0.95-1.20 Amps
Gun Anode Voltage	V_A	18.00-19.30 KV

TABLE I

4 PULSE ANALYSIS

We define "stable pulse" a pulse having a neat spectral line, as narrow as possible, without jumps in frequency (fig.5). A scan of the local oscillator frequency (60 ± 3 GHz) in a "stable" operating point of the gyrotron, showed that there were no other frequencies in that range.

For a stable pulse, the measured bandwidth (Full Width Half Maximum : FWHM) was about 300 KHz (±50 KHz) both at high (230 KW) and at low (50 KW) power.

For an instable pulse (fig. 6) the bandwidth was considerably larger (several MHz), the frequency varied rapidly during the pulse (even jumping) and the pulse breaked easily.

Instable pulses were obtained for particular setting of gyrotron parameters. For instance, in the high power (220KW) non distruptive 10 msec pulse of fig. 7, a frequency jump of 5 MHz is shown. When the scan time was not fast enough (1 msec in this case) two spikes appeared. A scan time of 0.2 msec was necessary to detect only one spectral line, indicating that the frequency jump appeared after 0.2 msec and before 1 msec with respect to the usual scan time. In this case also the direct frequency measurement (using a cavity wavemeter) showed the frequency jump.

For a correct gyrotron behaviour it is better to avoid these zones of instability.

5 FREQUENCY MEASUREMENTS ON GYROTRON # 011

Among the three tested gyrotron, this is the most stable, giving a continuous frequency variation for a change of the setting parameters. Assuming a frequency of 59.824 GHz for the usual working point, the frequency range 59.804-59.904 GHz has been explored.

5.1 Frequency and Power vs I_1 for different I_B

In fig. 8 power and frequency variations vs I_1 (Cavity Main Coil Current) for I_B = 6 Amps and 8 Amps are reported.
Frequency and power are higher for Beam Current I_B = 8 Amps. The f vs I_1 curves show an almost linear behaviour, confirming the "S" shape variation [6]. We could better say that there is a small ondulation of the frequency curve around a linear variation. Obviously for a main coil current increase there is a magnetic field increase and hence a frequency increase (as ω_c is proportional to B), and a power decrease. Linearizing the power decreasing rate, we could say that it has a negative slope of 1.21 MHz/KW.
The Δf Max (maximum frequency variation for one curve at I_B = const) is about 90 MHz.

5.2 Frequency vs V_A for different I_1

In fig. 9 is shown the frequency variation vs the Gun Anode Voltage for different values of I_1.
The curves tend to have a maximum for higher V_A at increasing I_1 values.
At I_1 = const the Δf Max is about 40 MHz.

5.3 Frequency vs I_2 for different I_1

The f vs I_2 curves shown in fig. 10 are monotonously growing, with the same slope as for the frequency variation due to a change in I_1 (-225 MHz/KG which corresponds at about 115 MHz/A). This result is understandable because I_1 and I_2 (currents in the cavity magnetic coils) have the same influence on the resonance frequency. The I_1 and

I_2 values are very similar, and as I_1 is chosen to increase power (at I_8 fixed), I_2 is used to optimize the shape of the magnetic gradient in the cavity. Thus if we change I_1 to choose the power, also I_2 has to be changed to optimize the efficiency of the interaction in the cavity. A small adjustment of I_2 is sufficient to maximize the output power for a given value of the other parameters.
The Δf Max at I_1 = const is about 30 MHz.

5.4 Frequency vs I_5 for different I_1

In fig. 11 is reported the frequency behaviour for a variation of I_5 at different I_1. Also in this case the curves show a maximum of the frequency, which is at higher values of I_5 for increasing I_1 values.
The Δf Max at I_1 = const is about 30 MHz.

5.5 Frequency vs Pulse-time

For fixed working parameters of the gyrotron in stable pulse operation, we have looked at the frequency variation during a pulse of 100 msec. The center scanning frequency was varied in a range of several MHz. Variation of the different frequency components of the pulse vs time were displaied on the spectrum analyser. The good stability of the power supply, allowed us to verify the correct reproductibility of pulses (for fixed parameters). Making a fast frequency scan, the error due to the drift of the I_8 was limited at about 1 MHz for the whole sequence of measurements.
In figs. 12, pictures of the appearing time of the different frequencies which composed the pulse are shown. In fig. 13 we have tried to summarize these results, giving in ordinate the gyrotron frequency (f gyrotron = f klystron + Δf beating) and in abscissa the appearing time during the pulse. The amplitude of the detected signal is reported for each frequency in dB. Even if the device is not power calibrated, a relative calibration between the amplitudes of the frequency signals shows, in a precise time, the percentage of each frequency.
It appears clearly that in the first 10 msec there is an increase in the significative values of frequency of 1.5 MHz . Then there is a

frequency decrease of 5.5 MHz. Such a frequency variation (6.10^6 / $60.10^9 \rightarrow - 10^{-4}$) is very small and ininfluent on the operation of the gyrotron. A first explanation of this complex time evolution of the frequency, could be both the finite time constant of the Anode Voltage which reaches the asymptotical value in about 10 msec (giving an increase of frequency) and the increasing cooling of the cathode during the pulse (giving a decrease of frequency). A contribution to this drift could also be found in contractions and dilatations of the cavity due to thermal effects which, changing slightly the geometrical dimensions produce an increase or a decrease of the frequency.

6 FREQUENCY MEASUREMENTS ON GYROTRON # 012

For this gyrotron we have obtained the following frequency variation range: 59.850 - 59.940 GHz (±60 MHz) with a frequency of 59.860 GHz for the usual working point.
In addition to the usual measurements with water load at the gyrotron exit (fig. 3), the calorimeter has been installed at the end of the transmission line, in the TE_{01} mode (fig. 4). Frequency measurements have been carried out at a constant I_B value, for separate variation of I_1, V_A and I_S .

6.1.1 Frequency and Power vs I_1 for different I_B

Also for this gyrotron an increase of I_1 produces a frequency increase and a power decrease with an average slope of 1.25 MHz/KW (fig. 14).

6.1.2 Frequency vs I_1 for different I_B : water load in the TE_{02} mode above the gyrotron

Looking into detail at the two frequency curves for I_B = 6 and 8 Amps (fig.15), we can see once again that they are almost parallel and show an "S" behaviour even in case of the frequency jump of about 30 MHz. The Δf Max was about 90 MHz.

6.1.3 Frequency vs I_1 at I_B =8 Amps, water load after the second bend of the transmission line, in the TE_{01} mode

On the average this curve (fig. 16) follows the identical one with water load in TE_{02}. It has a "big" frequency jump of ≈ 30 MHz at about the same I_1, but it has also three "small" jumps of ≈ 10 MHz. These jumps show clearly the influence of a mismatched line on the gyrotron behaviour. In fact 10 MHz corresponds to twice the distance between the gyrotron cavity and the water load (≈ 15 m). We know from burning papers and calorimetric power measurements, that this transmission line had a low efficiency (≈ 70 %).
Therefore we can think that spurious modes were created in the line, reflected by the water load (which is not adapted to these modes) and

have influenced the electron beam in the gyrotron cavity.
The "big" jump was not due to a mode changing, because the signal from the TE_{02} coupler did not show any variation. Maybe in the jumping zone this gyrotron works with electrical parameters which can cause an instability in the electron beam formation, giving a variation in the electrons speed distribution. Another explanation could be found in an excessive magnetic field tapering which could give rise to a saturating phenomenon of trapping for certain frequencies. When a critical value is reached, a relaxation of the saturation follows and the instability manifests itself in a frequency jump.
Summarizing, the "big" jump is probably due to an instability of the electron beam in the gyrotron, whilest the small jumps are due to a mismatch in the transmission line.

6.2.1 Frequency vs V_A for different I_1; water load in TE_{02} mode above the gyrotron

The curves (fig. 17) show a maximum in the frequency at increasing V_A values for higher I_1. "Big" frequency jumps (≈ 30 MHz) are present in a definite range of I_1 (18.20 - 18.30 Amps).
The Δf Max at I_1 = const is about 20 MHz without the jump and ≈ 55 MHz with the jump.

6.2.2 Frequency vs V_A for different I_1; water load in TE_{01} mode at the end of the line

On the average the curves (fig. 18) have a behaviour similar to the case without transmission line, having a maximum, and a jump of ≈ 30 MHz, but here there are small jumps (≈ 10 MHz) due to mismatches.

6.3 Frequency vs I_2 for different I_1; water load in TE_{02} mode above the gyrotron

A monotonous frequency increase is shown in fig. 19 for variation of I_2, with big jumps of about 30 MHz in a definite I_1 zone (18.10-18.20 Amps).
The Δf Max with I_1 = const is about 20 MHz without jump, and ≈ 50 MHz

with jump.

6.4.1 Frequency vs I_s for different I_1; water load in TE_{82} mode above the gyrotron

Curves with maximum are shown in fig. 20. For increasing I_1 values maxima are found at higher I_s. A big frequency jump is present for $I_1 = 18.30$.
The Δf Max at I_1 = const is about 20 MHz without jump and 40 MHz with jump.

6.4.2 Frequency vs I_s for different I_1; water load in TE_{01} mode at end of the line

The curves are rather flat (fig. 21), with a big jump of 30 MHz at almost equal I_s and small jumps of 10 MHz, due to mismatches in the line.

6.5 Frequency vs Pulse-time

The frequency evolution during the 100 msec pulse is shown in fig. 22. A variation of about 6.5 MHz has been detected. In the first 10 msec there is an increase of frequency, as shown in the detailed measurement reproduced in fig. 23. Later on, there is a frequency decrease.

6.6 Frequency vs Cathode Voltage

For this gyrotron we have checked that an increase of the Gun Anode Voltage corresponds to a decrease in the frequency, with an average slope of about 5 MHz/KV. The possibility of using this parameter to avoid the big frequency jump in a working zone of the gyrotron is effective. In fact, a frequency jump always leads to some trouble in the pulse. Therefore it is better to avoid this area. The measured small frequency variation ratio, ask for a large voltage variation to move sensitively the dangerous area.
As the Beam Voltage is fixed for all the set of gyrotrons, optimizing Vc for one source, we could influence negatively the behaviour of

another one. Therefore we have avoided to tune a gyrotron using this parameter. Luckily, our (maximum power) working range was rather far from this zone of instability, and no effective variation of Vc was needed.

7 FREQUENCY MEASUREMENTS ON GYROTRON # 013

For this gyrotron the frequency has been varied from 59.897 to 59.992 GHz (≃ 60 MHz) with an usual working point at 59.907 GHz. Measurements have been effectued for this gyrotron mounting the water load both directly above the source in the TE_{02} mode and at the end of the complete transmission line in the TE_{11} mode.

7.1.1 Frequency and Power vs I_1 for different I_8

An increase of I_1 gives an increase of frequency and a decrease of power with an average slope of 1.2 MHz/KW (fig. 24). The power has an anomalous increase both at I_8 = 8 and 6 Amps for the same I_1 value. In correspondence the frequency shows a jump of 40 MHz. We have to remark a pulse instability for I_1 values close to the jump ($I_1 < I_1$-jump). When I_1 tends to I_1-jump the spectral lines are larger and increase in number (fig. 25). Reducing the scan time we have detected in this zone a frequency jumping time smaller than 1 msec. For a further increase of I_1 ($I_1 > I_1$-jump) we found a stable pulse behaviour.

7.1.2 Frequency vs I_1 for different I_8; water load in TE_{02} mode above the gyrotron

The frequency increases with an "S" shape with a jump of 40 MHz (fig.26).
The Δf Max for I_8 = const is about 90 MHz (including the jump).

7.1.3 Frequency vs I_1 for different I_8; water load in TE_{11} at the end of the complete line

The frequency curves (fig.27) behave like for water load above the gyrotron. No other jumps are present. This means that the line is well matched, confirming the positive mode measurements with burning papers for this line.

7.2 Frequency vs V_A for different I_1

The curves (fig. 28) present an increasing maximum in V_A for higher I_1 values. Only one big jump of 40 MHz is present.
The Δf Max for I_1 = const is about 25 MHz excluding the jump, 60 MHz with jump.

7.3 Frequency vs I_2 for different I_1

These curves (fig. 29) increase monotously, and present two jumps of 40 MHz (I_1 = 17.80 - 17.90 Amps).
The Δf Max at I_1 = const is about 20 MHz, jump excluded, and 50 MHz, jump included.

7.4 Frequency vs I_5 for different I_1

These curves (fig. 30) show an increasing maximum in I_5 for higher I_1 values. There is an exception for the curve at I_1 = 17.90 Amps which shows two jumps of 40 and 30 MHz.
The Δf Max for I_1 = const is about 20 MHz (without jump) and 60 MHz with jump.

7.5 Frequency vs Pulse-time

The frequency evolution during a 100 msec pulse (fig.31), shows an increase (~ 1 MHz) of frequency in the first 5 msec and then a decrease of about 7 MHz.

8 CONCLUSIONS ON MEASUREMENTS

The principal results of the frequency measurements of the three gyrotrons are reported in table II.

The three gyrotrons showed the possibility of a frequency tuning of about 100 MHz for a standard working range. In this case the rate of power variation is on average -0.8 KW/MHz.

The frequency increases almost linearly ("S" shape curves) with the Main Coil Current (I_1 or I_2) at a rate of 200 MHz/KG . Two gyrotrons present a 30-40 MHz jump. This is probably due to a coupling process in the cavity rather than a mismatch due to the window, as in the case of the MIT 140 GHz gyrotron [6]. Large instabilities of the pulse are present for $I_1 < I_1$-jump. The presence of a transmission line can induce other small jumps of about 10 MHz if it is not well matched (creation of spurious modes and reflections).

Frequency curves for Gun Anode Voltage (V_A) and Cathode Current (I_5) variations, present maxima placed at higher V_A or I_5 values for higher I_1.

Big jumps (30-40 MHz) are present for the two mentioned gyrotrons. Small jumps (about 10 Mhz) are detected when there is a mismatch in the line.

It is possible to increase frequency, decreasing the Cathode Voltage (V_C) at a small rate of 5 MHz/KV. For long shots (~ 100 msec) a frequency increase (~ 1 MHz) has been measured at the beginning (0-10 msec) of the pulse. Later on, the frequency decreases of about 6 MHz. This frequency drift could be explained by a small variation in the value of the Beam Current (I_B) and/or by a small geometrical deformation of the cavity during the pulse.

For a stable pulse, a frequency bandwidth (FWHM) of about 300 KHz has been measured. When instabilities occur, the bandwidth broadens and the frequency tends to jump of several MHz in a time inferior to 1 msec.

	G # 011	G # 012	G # 013
absolute f range ±60 MHz	59.804-59.904 GHz	59.850-59.940 GHz	59.897-59.992 GHz
f work.	59.824 GHz	59.860 GHz	59.907 GHz
f and p vs I_s at I_s=8.6 A TE_{02}	>I_s >f S shape <P $\Delta f/\Delta P$~1.21 MHz/KW Δf_{Max}~90Mhz I_s cnst no big jumps no instabilities	>I_s >f S shape <P $\Delta f/\Delta P$~1.25 MHz/KW Δf_{Max}~90MHz I_s const big jump ~30MHz small instb I_1 <Ijump	>I_s >f S shape <P** $\Delta f/\Delta P$~1.20 MHz/KW Δf_{Max}~90MHz I_s const big jump ~40MHz large inst I_1 <Ijump
f vs I_1 ≠I_{WL} TEm_1	no measurements	WL TE_{01} :avrg.behavr like TE_{02} but small jumps ~10 MHz: line#2 mismatched	WL TE_{11} :avrg.behavr like TE_{02} -no jumps; line # 3 well matched
f vs V_A ≠I_{WL} TE_{02}	curves with Maxim. no jumps Δf_{Max}~10MHz I_1 cnst	curves with Maximum big jump ~ 30 MHz Δf_{Max} I_1 constant 30MHz(without jump) 55MHz(with jump)	curves with Maxim. big jump ~ 40 MHz Δf_{Max} I_1 constant 25MHz(without jump) 60MHz(with jump)
f vs V_A ≠I_{WL} TE_{01}	no measurements	average behaviour like TE_{02} small jumps ~ 10 MHz	no measurements
f vs I_2 ≠I_{WL} TE_{02}	>I_2 >f ΔI_1-$_2$/Δf~225MHz/KG no jumps Δf_{Max} I_1 constant ~ 30 MHz	>I_2 >f ΔI_1-$_2$/Δf~167MHz/KG big jumps ~ 30 MHz Δf_{Max} I_1 constant 20MHz(without jump) 50MHz(with jump)	>I_2 >f ΔI_1-$_2$/Δf~150MHz/KG big jumps ~40 MHz Δf_{Max} I_1 constant 20MHz(without jump) 50MHz(with jump)
f vs I_s ≠I_{WL} TE_{02}	curves with Maxim. no jumps Δf_{Max} I_1 constant	curves with Maximum big jump ~ 35 MHz Δf_{Max} I_1 constant 25MHz(without jump) 40MHz(with jump)	curves with Maximum big jumps~30&40MHz Δf_{Max} I_1 constant 20MHz(without jump) 90MHz(with jump)
f vs I_s ≠I_{WL} TE_{01}	no measurements	curves rather flat big jump ~ 30 MHz small jumps ~10 MHz	no measurements
f vs t 100 msec	t0-7msec Δf+1.5MHz t7-100ms Δf-6.5MHz	t0-10msec Δf+0.5MHz t10-100ms Δf-6.0MHz	t0-5msec Δf+1.0MHz t5-100ms Δf-5.0MHz
f vs V_c	no measurements	> V_c < f $\Delta f/\Delta V_c$ ~ 5 MHz/KV	no measurements

TABLE II

9 GYROTRON TUNING

We define as "stable working point" a long (~ 100 msec) high power (>200 KW) pulse, without breakdown, frequency jumps or other instabilities.

Up to now to find the optimal operational parameters of a gyrotron we based on direct frequency measurements on signals from the TE_{02} coupler and on calorimetric measurements to know the output power. Adding to these informations the knowledge of the safe working range given by the constructor we obtain an empirical recipe to tune a gyrotron. But it takes a certain time to calibrate a gyrotron in this way, and it could happen that the tube changes slightly its chracteristic after few months, thus we are obliged to calibrate it again. Besides, when we calibrate a gyrotron with the water load above it, we find operational parameters for that precise load. In this case it is very easy to obtain long-pulse shots even in presence of a discrete amount of spurious modes emitted by the gyrotron. But when we introduce a long and complex transmission line, problems appear. Often the line is not well matched. Spurious modes are produced and consequently reflected. This reflected power influence largely the gyrotron behaviour. In this case to tune a gyrotron for a long pulse shot, could be a very hard task. Anyway, once the line is mounted, we could think that the easiest way to work is to adapt the working point of the gyrotron at the line. Probably the truth is in the middle, between a correct mode control at the gyrotron exit and a matching of the gyrotron to the line. This could be shown using at the same time the gyro-radiometer to get informations from the gyrotron and the k-Spectrometer [9] to know modes in the line. Up to now we did not have the possibility to confirm this idea with an experiment.

10 METHOD OF THE MAXIMUM FREQUENCY AND POWER (MFP) FOR A STABLE WORKING POINT OF A GYROTRON

An empirical method to easily find the electrical parameters to tune a gyrotron in a stable working point , has been found using the gyro-radiometer.

This method, deduced from the frequency measurements of a gyrotron, has been successfully applied to another gyrotron, obtaining in a very short time, the complete set of working parameters. These were very close to the parameters deduced in a relatively long time from the direct frequency sample, the signals from the TE_{02} coupler, and from calorimetric power measurements.

The description of the method of the Maximum Frequency and Power (MFP) to tune a gyrotron is as follows.

First of all we have to note that a previous gyrotron calibration can be done installing above it, a matched load. In this case the source will be easier to tune, as there is no influence of the line on it.

A) The starting position is given by setting the principal electric parameters in the middle of the safe working zone indicated by the constructor. In this case we have:

$$I_1 = \underline{I}_1 \;;\; I_2 = \underline{I}_2 \;;\; I_S = \underline{I}_S \;;\; V_A = \underline{V}_A \;;\; V_C = \underline{V}_C \;;\; I_B = 8 \text{ Amps}$$

Than we have to vary, within its safety range, one parameter at a time keeping all the others constant, and measure the frequency variation using the gyro-radiometer.

B) I_1 (and eventually V_C) variation with $\underline{I}_2$, $\underline{V}_C$, $\underline{I}_S$, $\underline{V}_A$. If there is a big jump (several tens of MHz) in the characteristic of f vs I_1 we can deplace it varying V_C. Thus we will find a new V_C : $\rightarrow V_C^*$

C) I_S variation with $\underline{I}_1$, V_C^* , $\underline{I}_2$, $\underline{V}_A$. We will choose the I_S value which gives the maximum frequency $\rightarrow I_S^*$

D) V_A variation with $\underline{I}_1$, V_C^* , $\underline{I}_2$, I_S^* . We will keep the V_A^* value which gives the maximum frequency : $\rightarrow V_A^*$

E) I_1 variation with I_2, V_C^*, I_S^*, V_A^* . We will try to obtain the maximum (or the desired) power : → I_1^*

F) I_2 variation with I_1^*, V_C^*, I_S^*, V_A^* . We will try to maximize the desired power : → I_2^*

We can start again from C) to verify that the found parameters correspond at the criteria of maximum power and maximum frequency. We will have then obtained the following set of parameters:

$$I_1^* , I_2^* , I_S^* , V_A^* , V_C^*$$

which give a long and stable pulse. The corresponding power is almost the maximum available (sometimes few percent less).

We have to note that the parameters found with this method, are very close, if not identical, to those obtained using the previously described "recipe".

This method could interest constructors to verify the theoretically foreseen behaviour of gyrotrons, but it could surely be a great help for users, when they have to obtain high performances from the coupled system : gyrotron + transmission line.

In fact this method permits to find in a very short time the best gyrotron behaviour when matched with a complex transmission line. If the gyrotron losses its tuning, or the line is modified, using the MFP method, a new calibration demands a small waste of time. We could even think at a computer controlled system, based on the MFP method to find automatically the best working conditions. This could be indoubtly useful for large installations composed of 10 or more gyrotrons.

An improvement of the MFP method is necessary when we connect a transmission line to a gyrotron. In fact as we have seen, if the line is not perfect, it will be mismatched. To assure a stable behaviour of the source, we have to avoid the "troubled zone" induced by the mismatch. Therefore, if varying I_1 in the B) step, we note small frequency jumps of about 10 MHz, in the following steps : C),D),E),F), the optimum parameters will be those which give a detected frequency far enough from the small jumps (possibly equidistant two jumps).

11 A TENTATIVE OF EXPLANATION OF THE MFP METHOD

We try here to explain, using a simplified gyrotron theory, the empirically deduced MFP method.

When we maximize the power, we optimize the interaction of the resonant electrons in the cavity, shaping the magnetic field by mean of the Main Coil Currents I_1 and I_2 . In this way we produce a beam with the maximum power in the principal mode.

When we maximize the frequency we set the tube in a stable position (like for all the stationary points).

To confirm this intuitive position, we can look at the gyrotron behaviour from two points of view:

I) We can maximize the frequency, varying V_A and I_S, which have an influence on I_B, which has an influence on the frequency. Thus, varying indirectly the beam current, we vary $v_\parallel$ or the interaction time in the cavity N ($N = D/\lambda \cdot c/v_\parallel$, where D is the cavity length, λ the wavelength, c the speed of ligth and $v_\parallel$ the component of the electron velocity parallel to the axis). If we optimize the electron beam speed distribution, we optimize the interaction time (proportional to $v_\parallel$) and we could think that we meet a condition of maximum efficiency η , because

$$\eta = \frac{\eta^{\perp}}{1 + (v_\parallel / v^{\perp})^2}$$

where $\eta^{\perp}$, is the efficiency of energy extraction from the perpendicular component of the beam.

II) We can look at a gyrotron from an equivalent circuit point of view. Making an analogy with the klystron theory, we can schematize the equivalent circuit of an isolated cavity in the following way:

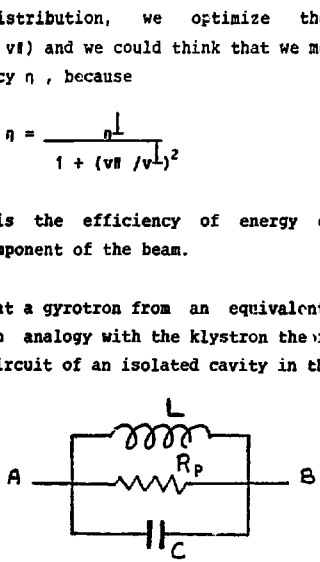

The fundamental equation of the cavity is:

$$L.C.\omega^2 = 1 \qquad ***$$

The ammettance betw-en A and B is:

$$Y = G + j.C.\omega - j/L.\omega$$

Considering now a gyrotron as a cavity, the presence of the elctron beam (which absorbs energy), introduces an admettance Yf:

$$Yf = Gf + j.Bf$$

Therefore the equivalent circuit becomes:

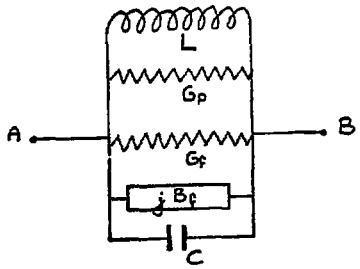

The total admettance is now:

$$Yf = G + Gf + j.C.\omega - j/L.\omega + j.Bf$$

Where Gf gives the losses in the cavity and Bf is the susceptance of the beam which varies with the transit angle θ ($\theta = \omega.t - \omega.D/v$).
As reguards the influence of the beam on the cavity, we establish an analogy with a klystron. We can see (fig. 32) that the beam introduces a susceptance which could be inductive or capacitive.
From the fundamental equation ***, when we maximize the frequency, we

decrease L or C, which means that we settle the parameters in order to work in the shown minimum of Bf.

Therefore exists a θ^* and hence a v_i^* which optimizes the energy exchange between the electrons and the RF field.

CONCLUSIONS

A precise measurement of the frequency of a gyrotron permits to avoid mismatches in the transmission line and to find optimal operational parameters.

A "Gyro-Radiometer" has been settled up for accurate frequency measurements of VARIAN 60 GHz gyrotrons. The possibility of tuning the frequency of these high power sources within 100 MHz, in a safety range has been verified.

A bandwidth of ~ 300 KHz (FWHM) has been measured.

A frequency drift of ~ 6 - 7 MHz has been observed in 100 msec pulses. Frequency variations for different settings of the principal gyrotron electric parameters have shown interesting features. The almost linear frequency variation with the Main Coil Currents has been verified. Curves having a maximum, are representative of Anode Voltage and Cathode Current variations. Some sources showed sudden high frequency jumps (~ 40 MHz) with instable pulses. During these instable pulses, fast (< 1 msec) frequency variations (few MHz) and larger bandwidth, were detected.

When the gyrotrons were connected to a transmission line, small frequency jumps (~ 10 MHz) occurred if the line was not well matched. This influence of the load on the source behaviour has to be taken into account when tuning a gyrotron for a high power, long and stable pulse.

A method (MFP) for a fast and optimal gyrotron tuning has been found. The use of this system permits to obtain in a very short time, a stable-long pulse, at any choose power value without knowing any setting parameter, and whatever the load is. For any working condition, even at maximum power, a stable pulse is obtained in correspondence of a maximum of the emitted frequency.

ACKNOWLEDGEMENTS

The author wishes to thank Drs. S.Cirant, J.P.Crenn, G.Mourier, B.Tournesac for helpful discussions; the FOM-ECRH Team and J.M. Chareau for technical help.

APPENDIX

The measurement with the gyro-radiometer confirmed the possibility of an easy frequency tuning in a discrete range.

Among the parameters which could have an influence on the frequency behaviour of a gyrotron, the Anode Voltage has the lowest reaction time. We could use this possibility of a fast electrical variation, to stabilize the frequency of the source. A fast and precise frequency detection could give a signal which will be subtracted from a stable reference one. The difference, once amplified, should act as feedback for the Anode Voltage control system.

A typical value of the frequency drift which could be controlled is about 5 MHz / 100 msec.

Phase locked gyrotrons could be of greater physics and technological interest. In fact, phase controlled sources could permit the use of phased array antennae, and other physics employs.

In a f'rst study to lock the phase of a gyrotron, a discrete power is needed as input to control the phase [10].

We think that an easier scheme, similar to the frequency control one, could permit a phase control. A fast detection of the gyrotron phase, compared with a stabilized reference source, could give a feedback signal to the Anode Voltage control system. The fast influence of this parameter on the gyrotron behaviour should assure a good phase coherence.

A first experiment of phase detection, based on the beating of a centimetric phase-locked source with a gyrotron signal, was lately performed.

Using an advanced microwave measurements set up [11] we were able to detect accurately the frequency spectrum of the #012 gyrotron, for a pulse of 10 msec and 220 KW of output power (fig.33). Two "wings" appeared 35 dB below the central spectral line, 1 MHz aside. Other peaks were lower than 50 dB. This gyrotron showed, with respect to the locked L.O., a good stability and high reproductibility of pulses. These aspects were confirmed by phase detection. In this case the beating signal was sent to a digital scope. The variation of the sinusoidal curve of the beating (beating frequency of about 60 MHz) gave informations about the phase change. Rather surprisingly the

sinusoid was remarkably stable and clear. Fig 34 a and b show a 90^0 phase variation after 6 pulses (detected almost at the end of the pulse). Thus, even if this gyrotron was unlocked, it showed an "intrinsic" phase stability of 15^0/pulse.

In the same experience, stability of the klystron precedently used has been tested. A measured frequency drift of 10 MHz/h allows us to exclude this source to be responsable of influences in the measurements of gyrotron frequency evolution. The klystron frequency spectrum is shown in fig. 35.

ACKNOWLEDGEMENT

The author wishes to thank Dr. P. Goy for the use of his microwave device during this last experience.

FIGURE CAPTIONS

Fig. 1 a,b Schematic diagrams of a gyrotron oscillator

Fig. 2 Schematic diagram of the Gyro-Radiometer

Fig. 3 Set up for frequency measurements with water load above the gyrotron

Fig. 4 Set up for frequency measurements with water load at the end of the transmission line

Fig. 5 "Stable pulse" spectral line

Fig. 6 "Instable pulse" spectral line

Fig. 7 Instable pulse - frequency jump

Fig. 8 # 011 f and P vs I_1 I_B = 6,8 Amps

Fig. 9 # 011 f vs V_A different I_1

Fig.10 # 011 f vs I_2 different I_1

Fig.11 # 011 f vs I_5 different I_1

Fig.12 # 011 Pictures of the appearing time for different frequencies during the pulse

Fig.13 # 011 Gyrotron frequency f vs Pulse-time t . 0-100 msec.

Fig.14 # 012 f and P vs I_1 I_B = 6,8 Amps

Fig.15 # 012 f vs I_1 different I_B - TE_{02}

Fig.16 # 012 f vs I_1 I_B = 8 A - TE_{01}

Fig.17 # 012 f vs V_A different I_1 - TE_{02}

Fig.18 # 012 f vs V_A different I_1 - TE_{01}

Fig.19 # 012 f vs I_2 different I_1 - TE_{02}

Fig.20 # 012 f vs I_5 different I_1 - TE_{02}

Fig.21 # 012 f vs I_5 different I_1 - TE_{01}

Fig.22 # 012 Gyrotron frequency f vs Pulse-time t . 0-100 msec.

Fig.23 # 012 f vs t . 0-10 msec.

Fig.24 # 013 f and P va I_1 I_B = 6,8 Amps

Fig.25 # 013 pulse instabilities for $I_1 < I_1$-jump

Fig.26 # 013 f vs I_1 different I_B - TE_{02}

Fig.27 # 013 f vs I_1 different I_B - TE_{11}

Fig.28 # 013 f vs V_A different I_1 - TE_{02}

Fig.29 # 013 f vs I_2 different I_1 - TE_{02}

Fig.30 # 013 f vs I_5 different I_1 - TE_{02}

Fig.31 # 013 Gyrotron frequency f vs Pulse-time t . 0-100 msec .

Fig.32 Electron beam susceptance introduced in the reasonance cavity

Fig.33 # 012 gyrotron frequency spectrum t=10 msec P=220 KW

Fig.34 a,b 90^0 phase variation after 6 pulses

Fig.35 klystron frequency spectrum

REFERENCES

[1] V.A.Flyagin, A.V.Gaponov, M.I.Petelin, V.K.Yulpatov : "The Gyrotron" IEEE Transactions Microwave Theory and Techniques Vol MTT-25 N° 6 pp 514-521 June 1977.

[2] G.Mourier : "Gyrotron tubes - A Theoretical Study" Archiv fur Elektronik und Ubertragungstechnik Band 34 pp 473-484 1980.

[3] J.L.Hirshfield, V.l.Granatstein : "The Electron Cyclotron Maser - An Historical Survey" IEEE Transactions Microwave Theory and Techniques Vol Mtt - 25 N° 6 pp 522-527 June 1977.

[4] R.S.Symons, H.R.Jory : "Cyclotron Resonance Devices" Adv. in Electron Elect. Phys. 55 pp 235-240 1981.

[5] VARIAN comunication presented at the DOE Gyrotron User/Developer Meeting held in Germantown , MD April 1982.

[6] K.E.Kreischer, B.G.Danly, P.Woskoboinikow, W.J.Mulligan, R.J.Temkin : "Frequency pulling and bandwidth measurement of a 140 GHz pulsed gyrotron" Int. J. Electronics Vol 57 N° 6 pp 851-862 1984.

[7] HUGHES comunication presented at the DOE Gyrotron User/Developer Meeting held in Germantown , MD April 1982.

[8] G.F.Brand, N.G.Douglas, M.Grass, J.Y.L.May Chen Zhiyi : "Frequency Detuning Measurements in a Low-Power Gyrotron" Int. J. Electronics Vol 57 N° 6 pp 891-900 1984.

[9] W.Kasparek, G.A.Muller : "A Novel Device for Multimode Analysis in Oversized Waveguides" Digest 10th Int. Conference on Infrared and Millimiter Waves

Lake Buena Vista pp 238-239 December 1985.

[10] M.E.Read, R.Seeley, W.M.Manheimer : "Observation of Phase Locking in a Single-Cavity Gyrotron Oscillator"
IEEE Trans. on Plasma Science, Vol PS-13 N° 6 pp 398-403
December 1985.

[11] P.Goy, M.Gross, C.Mauc : "Un banc millimetrique de 27 a 110 GHz complet, simple et economique"
L' Onde electrique 1986. (To be published)

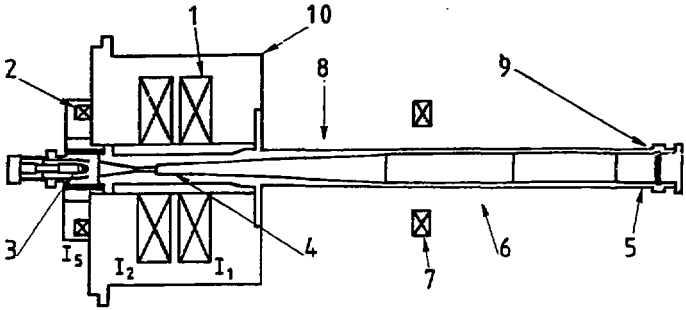

1- Main magnet coils
2- Gun magnet coil
3- Electron gun
4- Cavity
5- Output waveguide and window
6- Beam collector area
7- Collector magnet coils
8- Output guide up-transition
9- Single window
10- Dewar

Fig. 1a

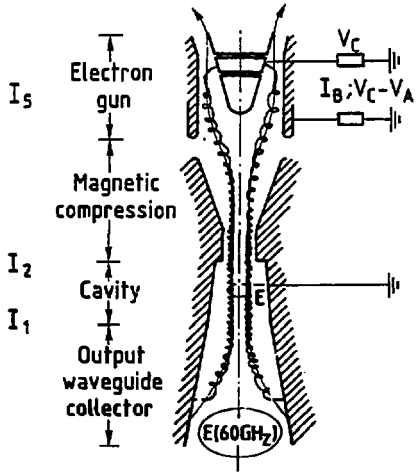

Fig. 1b

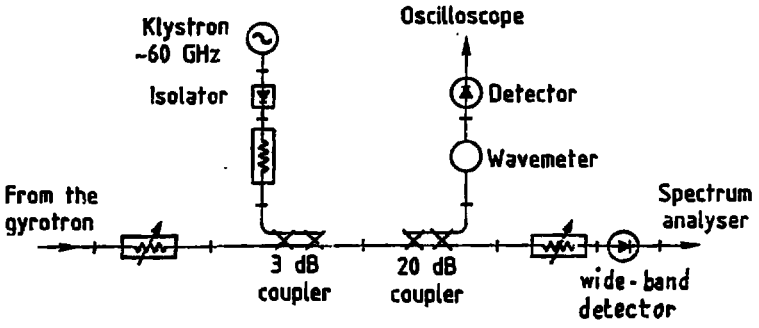
Klystron
~60 GHz
Isolator
Oscilloscope
Detector
Wavemeter
From the
gyrotron
Spectrum
analyser
3 dB
coupler
20 dB
coupler
wide-band
detector

Fig. 2

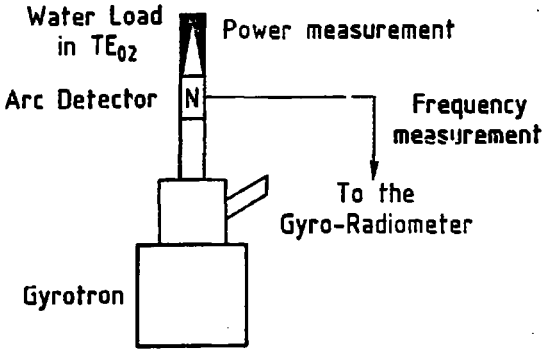
Water Load
in TE_{02}
Power measurement
Arc Detector
N
Frequency
measurement
To the
Gyro-Radiometer
Gyrotron

Fig. 3

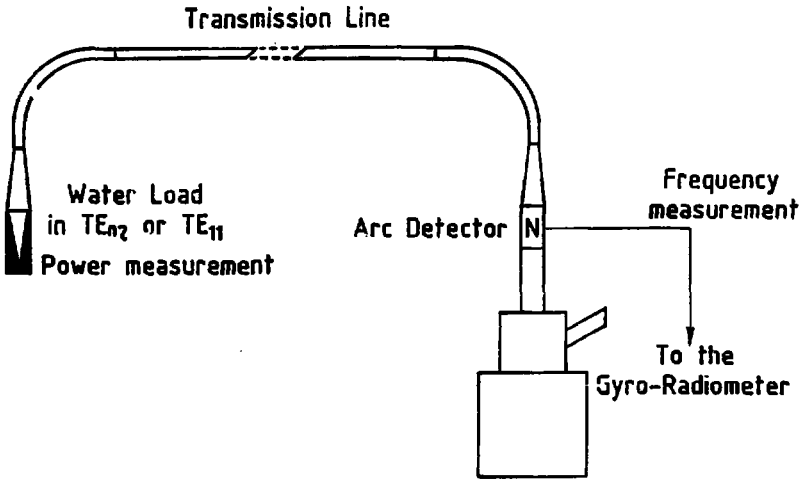
Transmission Line
Water Load
in TE_{02} or TE_{11}
Power measurement
Arc Detector
N
Frequency
measurement
To the
Gyro-Radiometer

Fig. 4

1 MHz/div

Linear

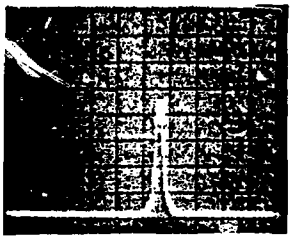

013
Stable Pulse

Fig. 5

2 MHz 2 MHz

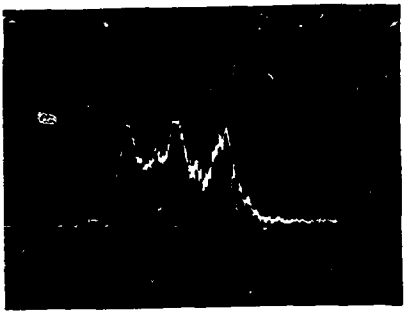

013
Instable Pulse

Fig. 6

5 MHz

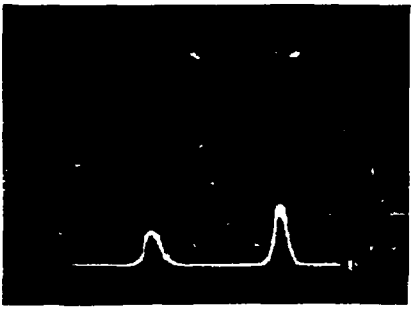

013
Frequency jump

Fig. 7

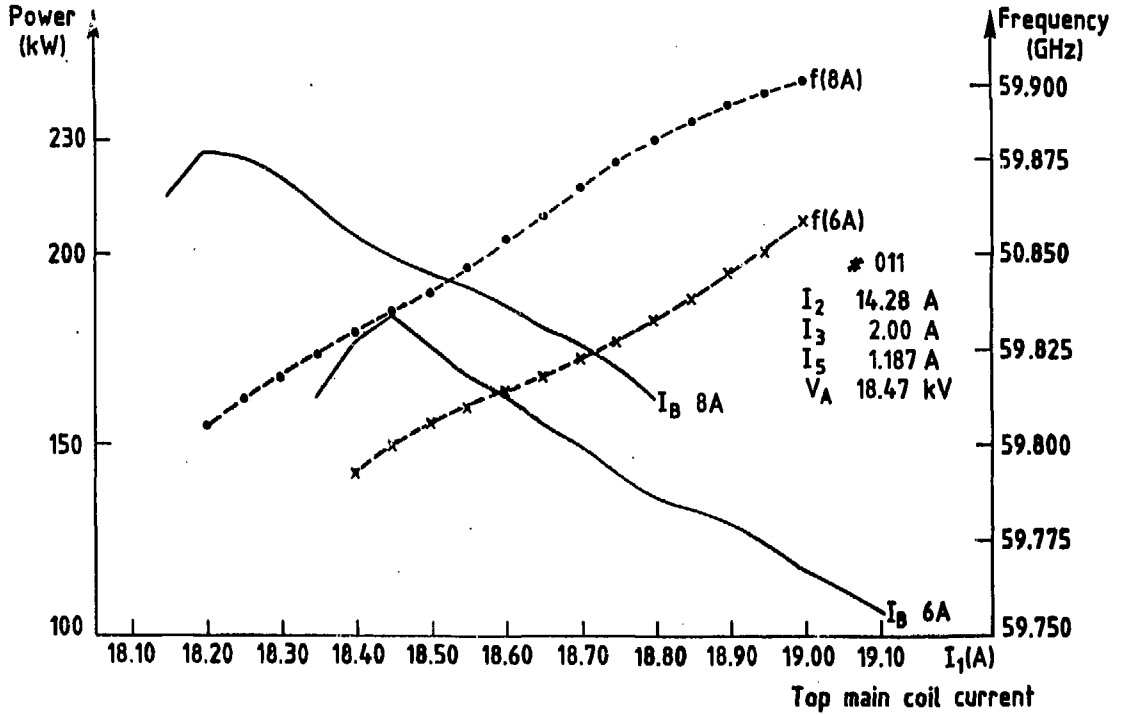
Power
(kW)
Frequency
(GHz)
230
200
150
100
59.900
59.875
50.850
59.825
59.800
59.775
59.750
f(8A)
f(6A)
# 011
I_2 14.28 A
I_3 2.00 A
I_5 1.187 A
V_A 18.47 kV
I_B 8A
I_B 6A
18.10
18.20
18.30
18.40
18.50
18.60
18.70
18.80
18.90
19.00
19.10
I_1(A)
Top main coil current

Fig. 8

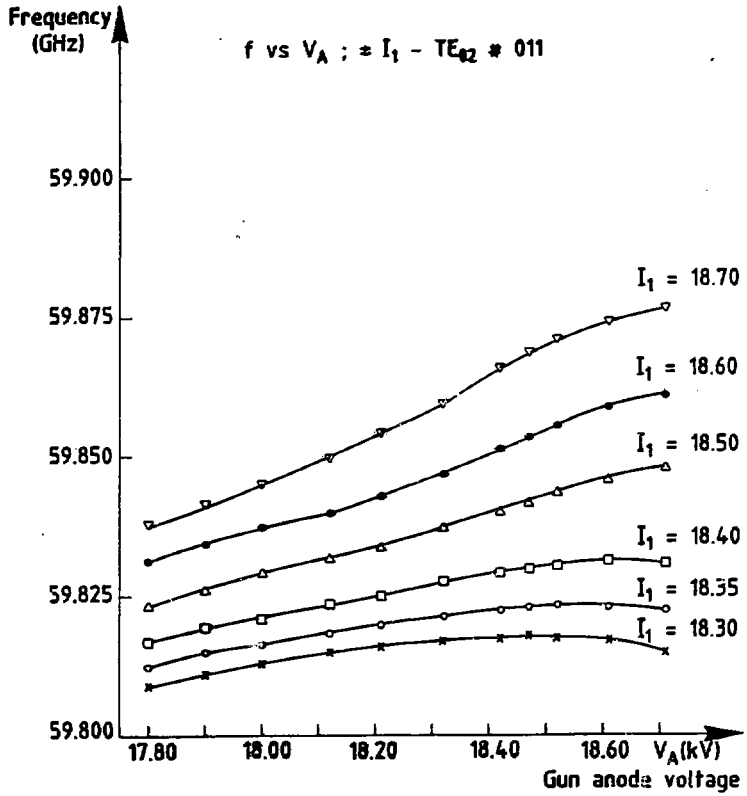
Frequency (GHz)
f vs V_A ; ± I_1 - TE_{62} # 011
59.900
59.875
59.850
59.825
59.800
I_1 = 18.70
I_1 = 18.60
I_1 = 18.50
I_1 = 18.40
I_1 = 18.35
I_1 = 18.30
17.80
18.00
18.20
18.40
18.60
V_A(kV)
Gun anode voltage

Fig. 9

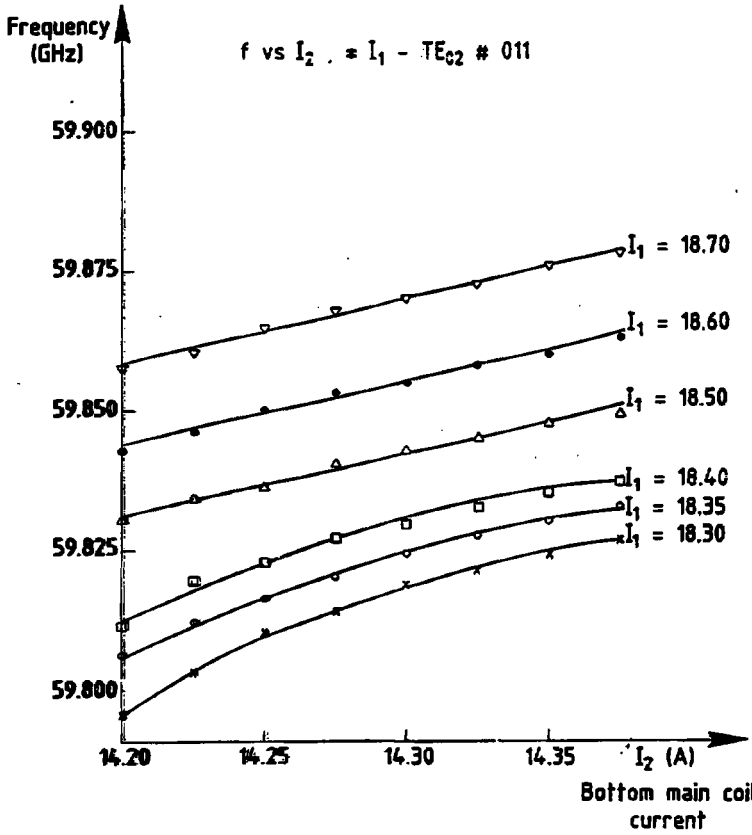
Frequency (GHz)
f vs I_2 , I_1 - TE_{02} # 011
59.900
59.875
59.850
59.825
59.800
I_1 = 18.70
I_1 = 18.60
I_1 = 18.50
I_1 = 18.40
I_1 = 18.35
I_1 = 18.30
14.20
14.25
14.30
14.35
I_2 (A)
Bottom main coil current

Fig. 10

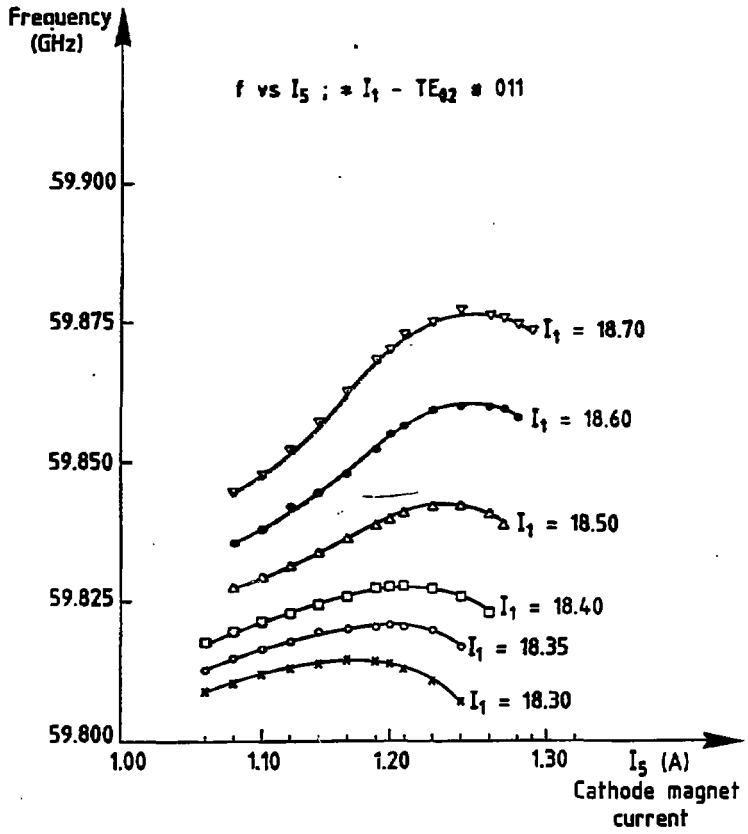
Frequency (GHz)
f vs I_5 ; * I_1 - TE_{82} * 011
59.900
59.875
59.850
59.825
59.800
I_1 = 18.70
I_1 = 18.60
I_1 = 18.50
I_1 = 18.40
I_1 = 18.35
I_1 = 18.30
1.00
1.10
1.20
1.30
I_5 (A)
Cathode magnet current

Fig. 11

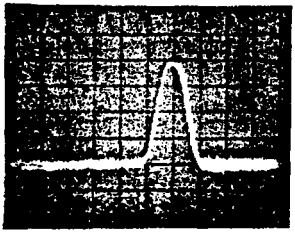

i f = 59.917 GHz

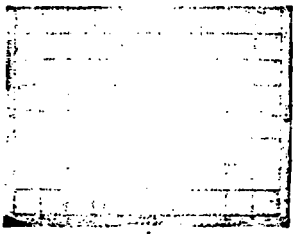

j f = 59.916(5) GHz

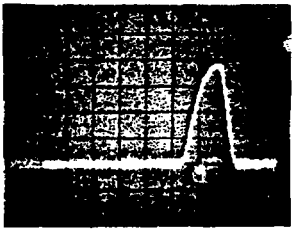

k f = 59.916 GHz

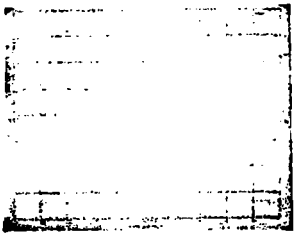

l f = 59.915(5) GHz

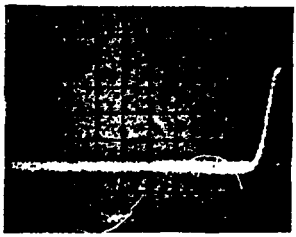

m f = 59.915 GHz

n f = 59.914(5) GHz

Fig. 12

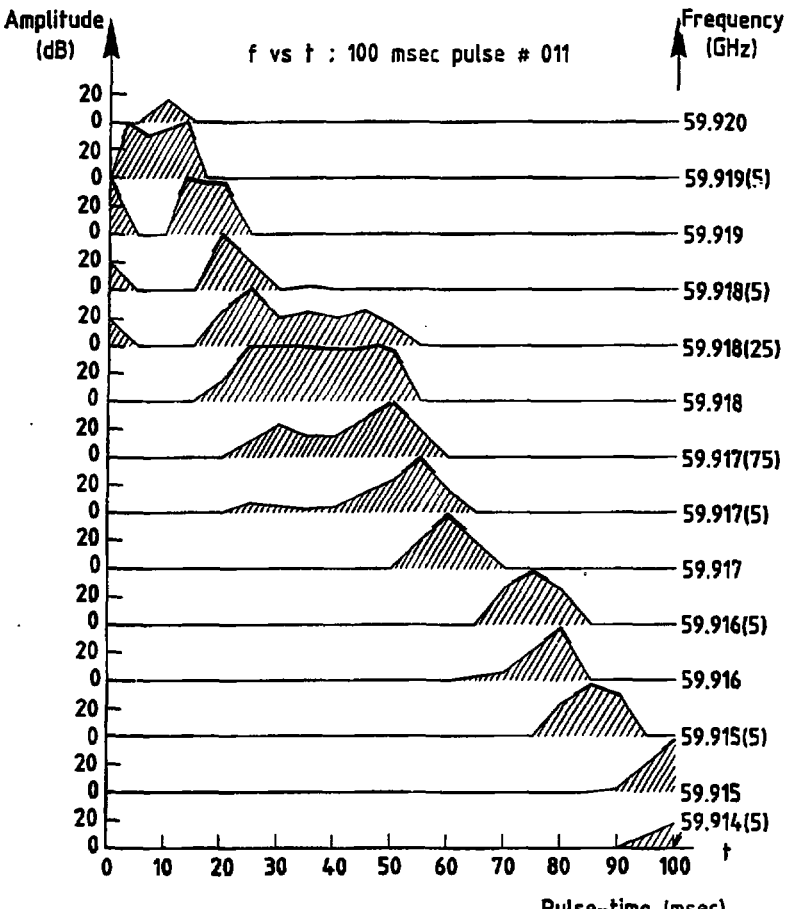
Amplitude
(dB)
f vs t : 100 msec pulse # 011
Frequency
(GHz)
20
0
59.920
59.919(5)
59.919
59.918(5)
59.918(25)
59.918
59.917(75)
59.917(5)
59.917
59.916(5)
59.916
59.915(5)
59.915
59.914(5)
0 10 20 30 40 50 60 70 80 90 100
t
Pulse-time (msec)

Fig. 13

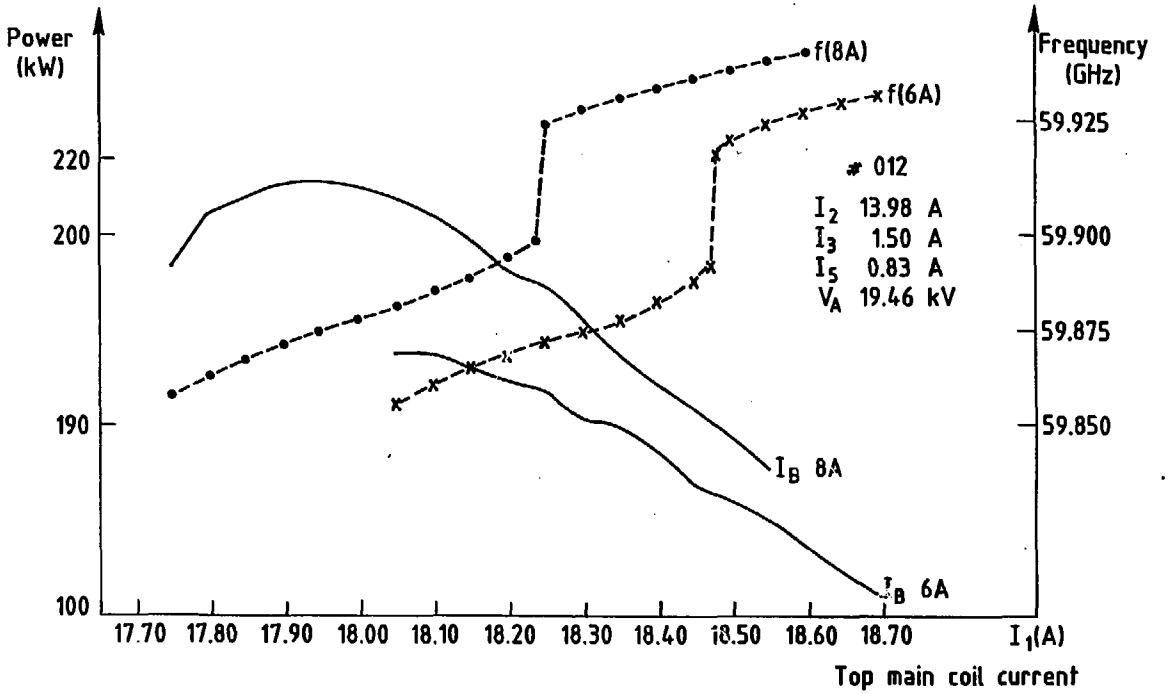
Power
(kW)
220
200
190
100
Frequency
(GHz)
59.925
59.900
59.875
59.850
f(8A)
f(6A)
# 012
I_2 13.98 A
I_3 1.50 A
I_5 0.83 A
V_A 19.46 kV
I_B 8A
I_B 6A
17.70 17.80 17.90 18.00 18.10 18.20 18.30 18.40 18.50 18.60 18.70
I_1(A)
Top main coil current

Fig. 14

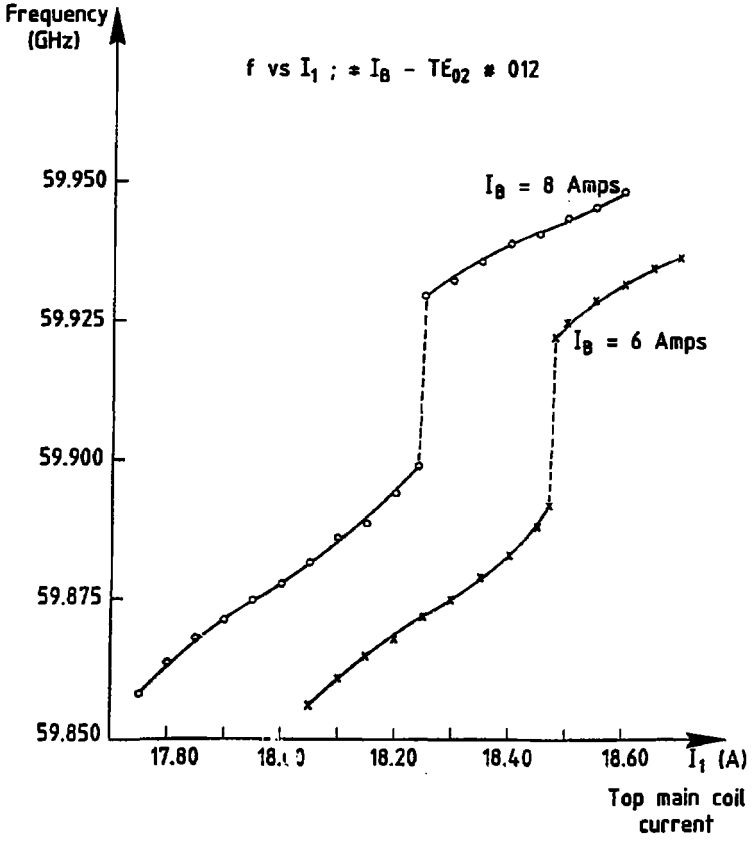
Frequency (GHz)
f vs I_1 ; * I_B - TE_{02} * 012
59.950
59.925
59.900
59.875
59.850
I_B = 8 Amps
I_B = 6 Amps
17.80
18.20
18.40
18.60
I_1 (A)
Top main coil current

Fig. 15

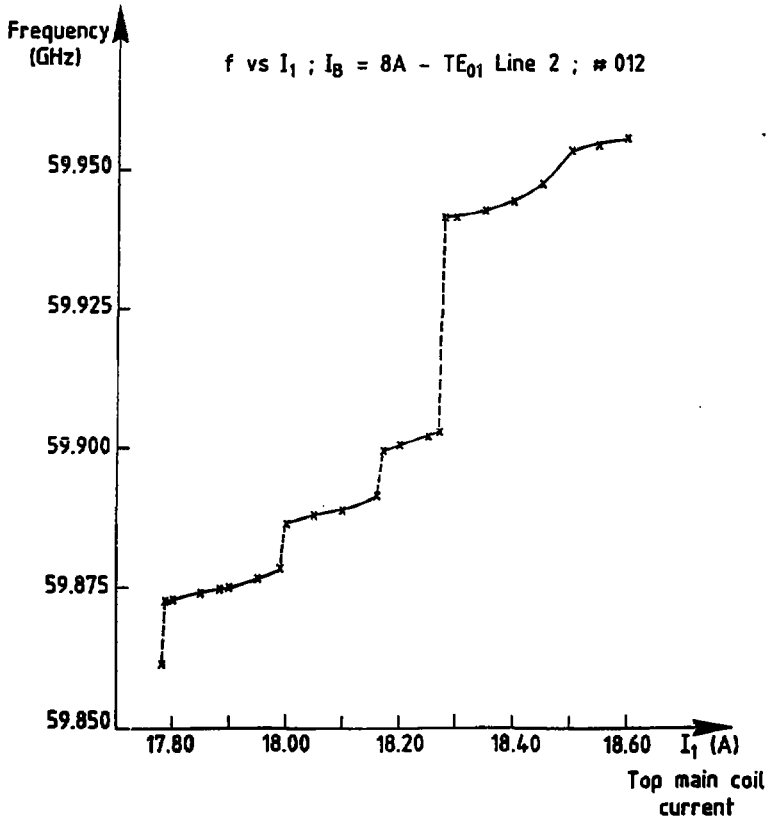
Frequency (GHz)
f vs I_1 ; I_B = 8A - TE_{01} Line 2 ; # 012
59.950
59.925
59.900
59.875
59.850
17.80
18.00
18.20
18.40
18.60
I_1 (A)
Top main coil current

Fig. 16

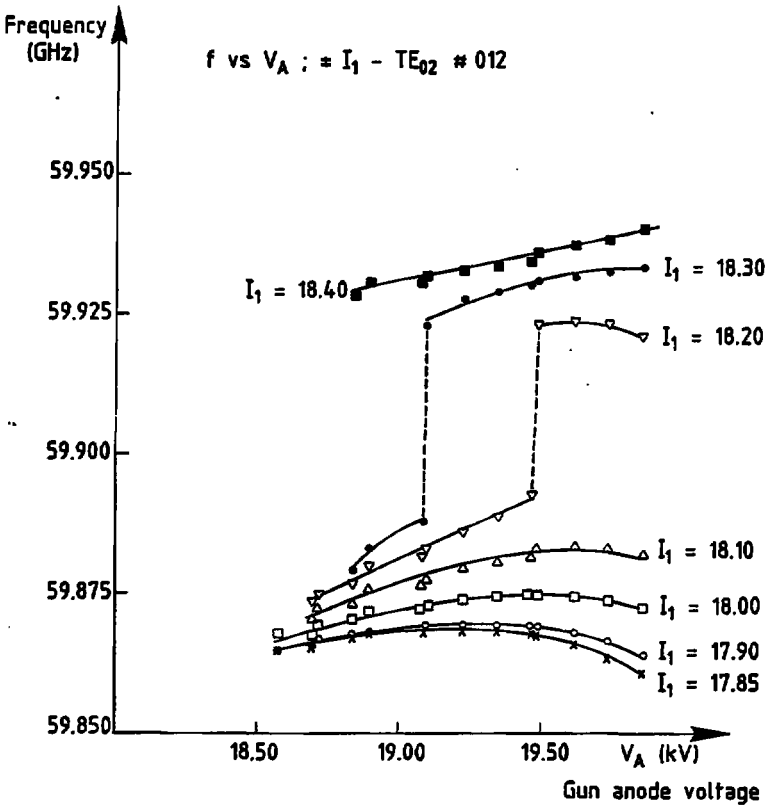
Frequency
(GHz)
f vs V_A ; ≈ I_1 - TE_{02} ≈ 012
59.950
59.925
59.900
59.875
59.850
I_1 = 18.40
I_1 = 18.30
I_1 = 18.20
I_1 = 18.10
I_1 = 18.00
I_1 = 17.90
I_1 = 17.85
18.50
19.00
19.50
V_A (kV)
Gun anode voltage

Fig. 17

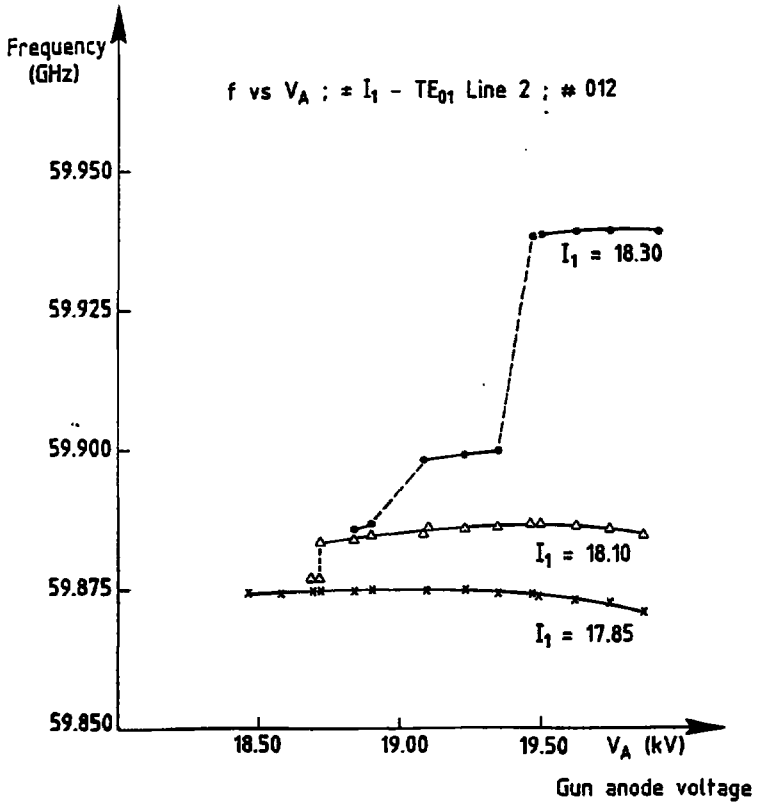
Frequency
(GHz)
f vs V_A ; ∗ I_1 - TE_{01} Line 2 ; # 012
59.950
59.925
59.900
59.875
59.850
I_1 = 18.30
I_1 = 18.10
I_1 = 17.85
18.50
19.00
19.50
V_A (kV)
Gun anode voltage

Fig. 18

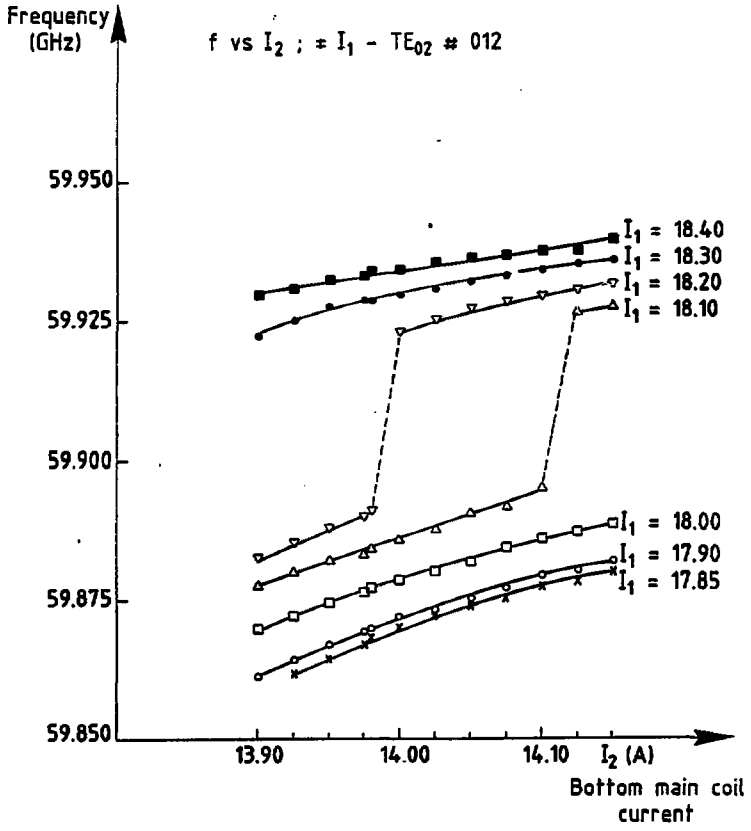
Frequency (GHz)
f vs I_2 ; ≠ I_1 - TE_{02} # 012
59.950
59.925
59.900
59.875
59.850
I_1 = 18.40
I_1 = 18.30
I_1 = 18.20
I_1 = 18.10
I_1 = 18.00
I_1 = 17.90
I_1 = 17.85
13.90
14.00
14.10
I_2 (A)
Bottom main coil current

Fig. 19

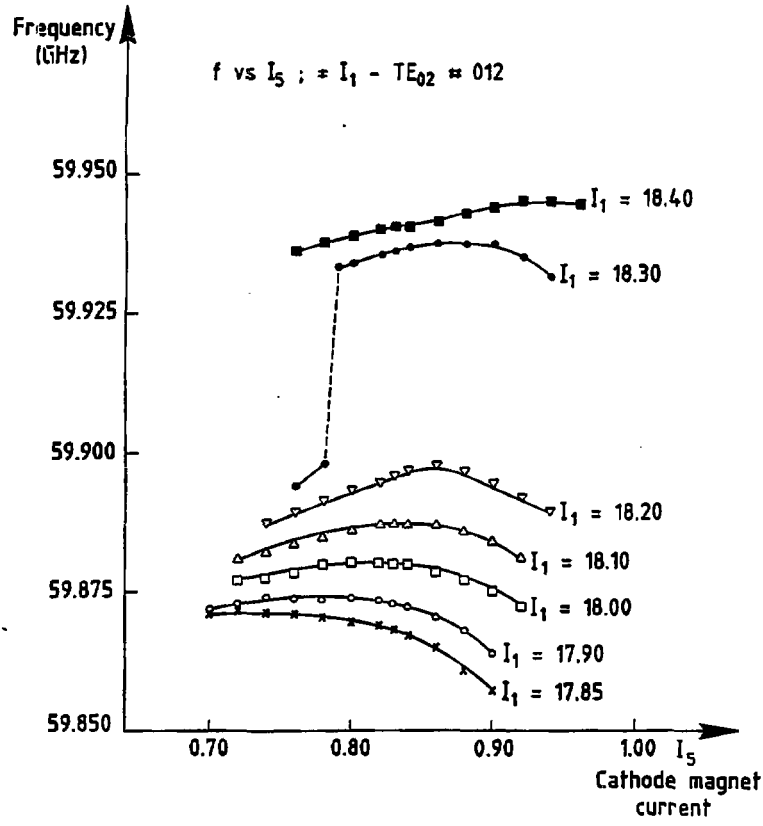
Frequency (GHz)
f vs I_5 ; * I_1 - TE_{02} * 012
59.950
59.925
59.900
59.875
59.850
I_1 = 18.40
I_1 = 18.30
I_1 = 18.20
I_1 = 18.10
I_1 = 18.00
I_1 = 17.90
I_1 = 17.85
0.70
0.80
0.90
1.00
I_5
Cathode magnet current

Fig. 20

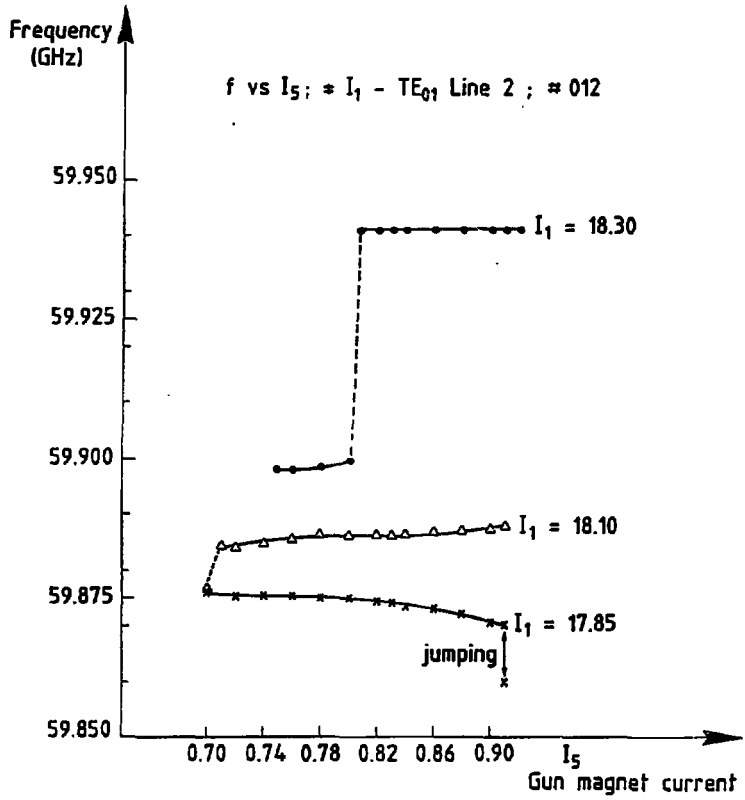
Frequency (GHz)
f vs I_5 ; ≠ I_1 - TE_{01} Line 2 ; ≠ 012
59.950
59.925
59.900
59.875
59.850
I_1 = 18.30
I_1 = 18.10
I_1 = 17.85
jumping
0.70 0.74 0.78 0.82 0.86 0.90
I_5
Gun magnet current

Fig. 21

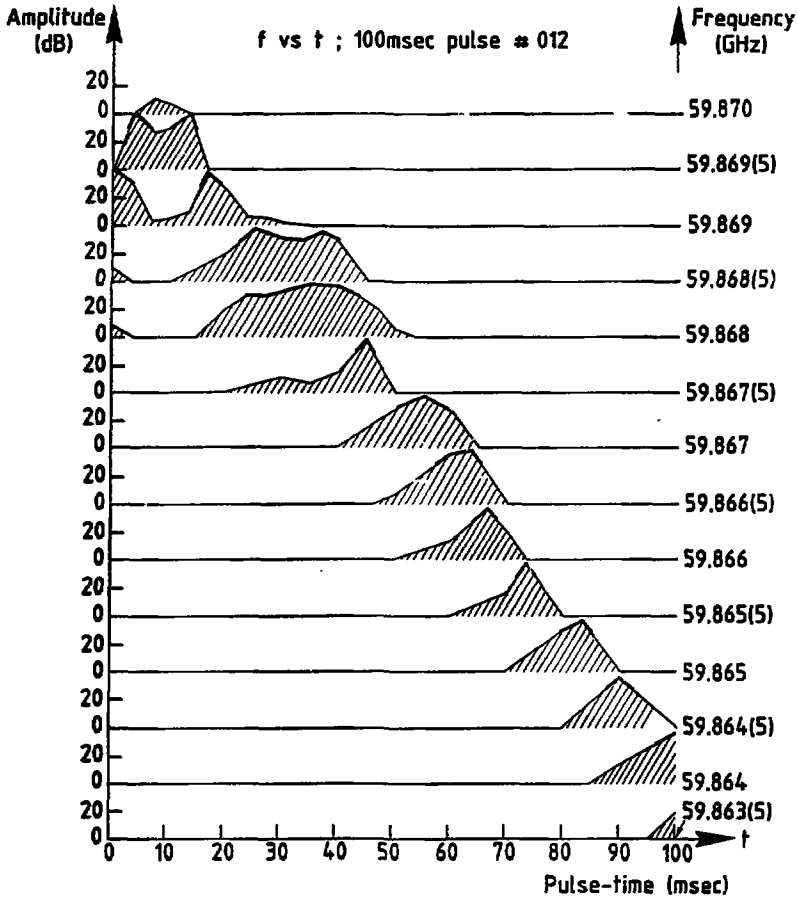
Amplitude (dB)
f vs t ; 100msec pulse # 012
Frequency (GHz)
20
0
59.870
59.869(5)
59.869
59.868(5)
59.868
59.867(5)
59.867
59.866(5)
59.866
59.865(5)
59.865
59.864(5)
59.864
59.863(5)
0 10 20 30 40 50 60 70 80 90 100
t
Pulse-time (msec)

Fig. 22

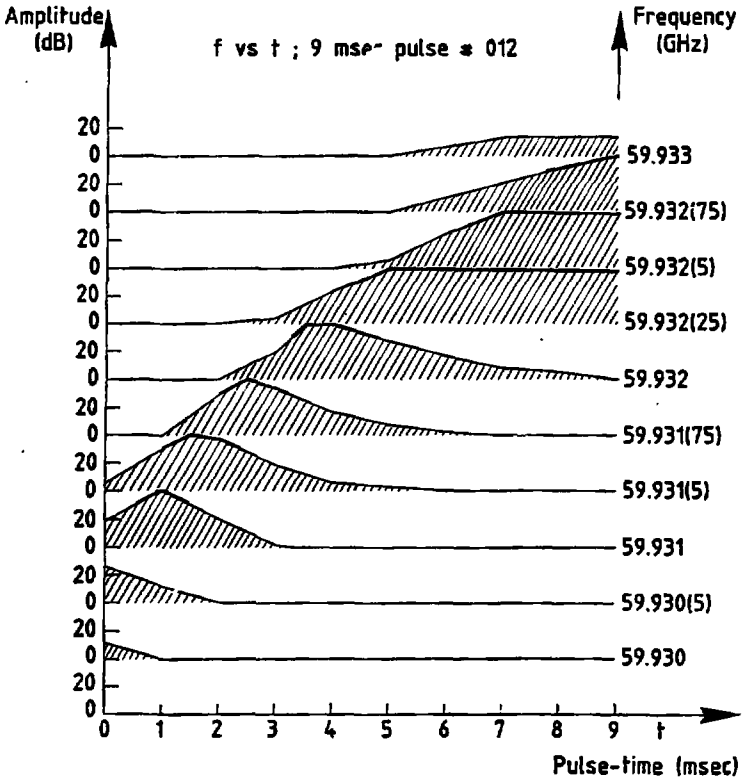
Amplitude
(dB)
f vs t ; 9 msec pulse ≈ 012
Frequency
(GHz)
20
0
59.933
59.932(75)
59.932(5)
59.932(25)
59.932
59.931(75)
59.931(5)
59.931
59.930(5)
59.930
0 1 2 3 4 5 6 7 8 9 t
Pulse-time (msec)

Fig. 23

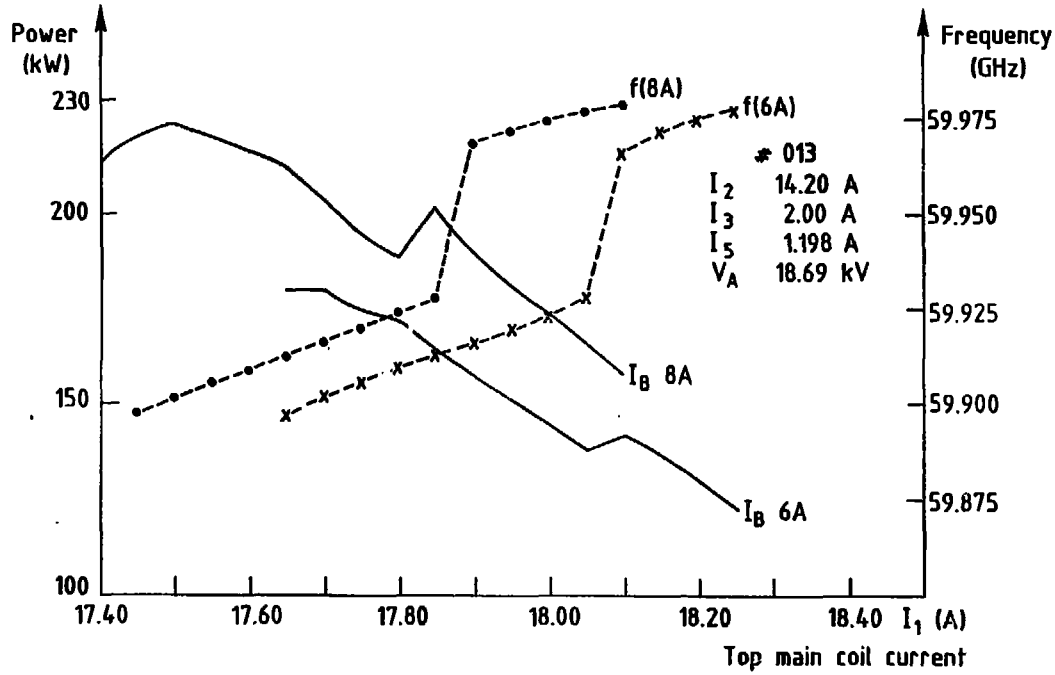
Power
(kW)
230
200
150
100
Frequency
(GHz)
59.975
59.950
59.925
59.900
59.875
f(8A)
f(6A)
# 013
I_2 14.20 A
I_3 2.00 A
I_5 1.198 A
V_A 18.69 kV
I_B 8A
I_B 6A
17.40
17.60
17.80
18.00
18.20
18.40
I_1 (A)
Top main coil current

Fig. 24

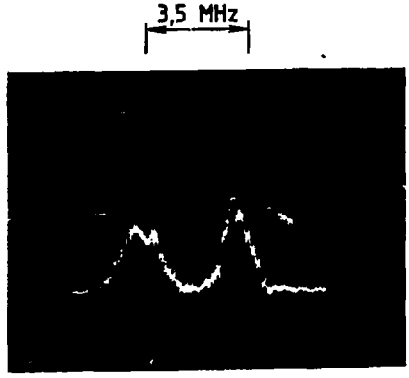

Fig. 25

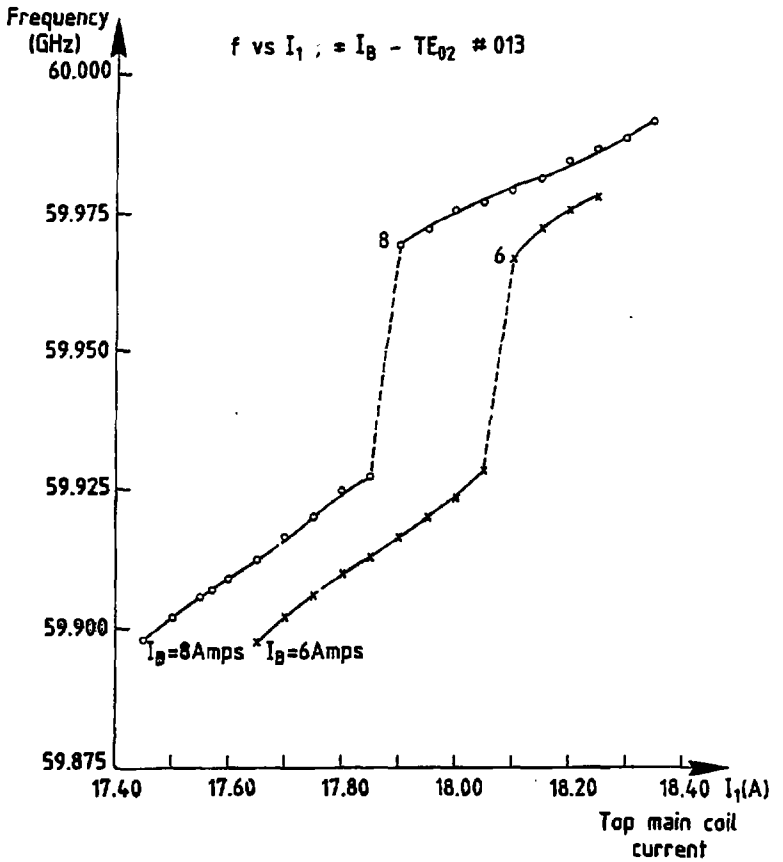
Frequency
(GHz)
f vs I_1 ; ≡ I_B - TE_{02} # 013
60.000
59.975
59.950
59.925
59.900
59.875
8
6
I_B=8Amps
I_B=6Amps
17.40
17.60
17.80
18.00
18.20
18.40
I_1(A)
Top main coil
current

Fig. 26

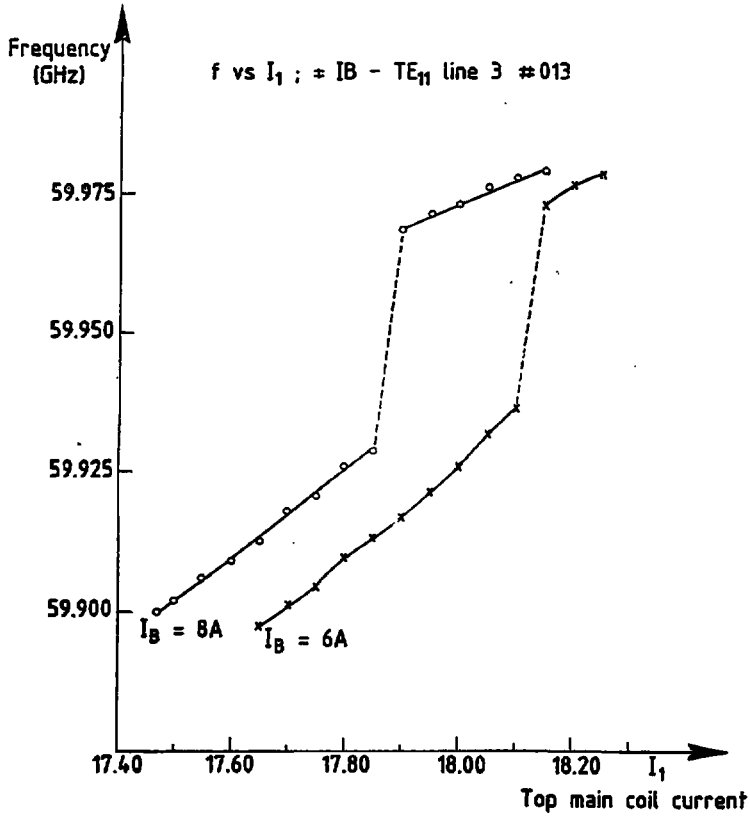
Frequency
(GHz)
f vs I_1 ; ≠ IB - TE_{11} line 3 #013
59.975
59.950
59.925
59.900
I_B = 8A
I_B = 6A
17.40
17.60
17.80
18.00
18.20
I_1
Top main coil current

Fig. 27

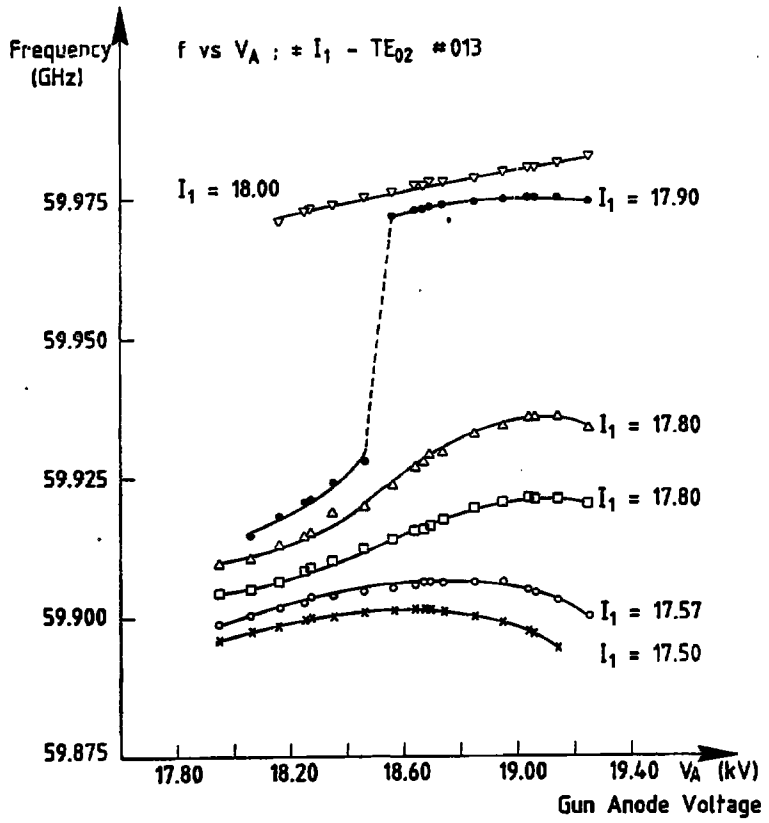
Frequency (GHz)
f vs V_A ; I_1 - TE_{02} #013
I_1 = 18.00
I_1 = 17.90
I_1 = 17.80
I_1 = 17.80
I_1 = 17.57
I_1 = 17.50
59.975
59.950
59.925
59.900
59.875
17.80
18.20
18.60
19.00
19.40
V_A (kV)
Gun Anode Voltage

Fig. 28

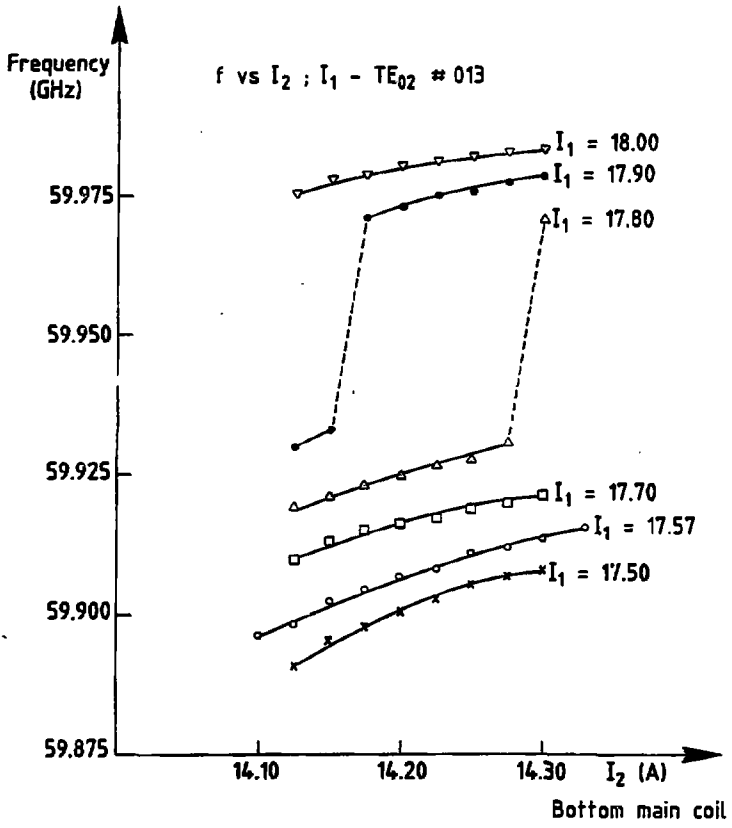
Frequency
(GHz)
f vs I_2 ; I_1 - TE_{02} # 013
I_1 = 18.00
I_1 = 17.90
I_1 = 17.80
I_1 = 17.70
I_1 = 17.57
I_1 = 17.50
59.975
59.950
59.925
59.900
59.875
14.10
14.20
14.30
I_2 (A)
Bottom main coil

Fig. 29

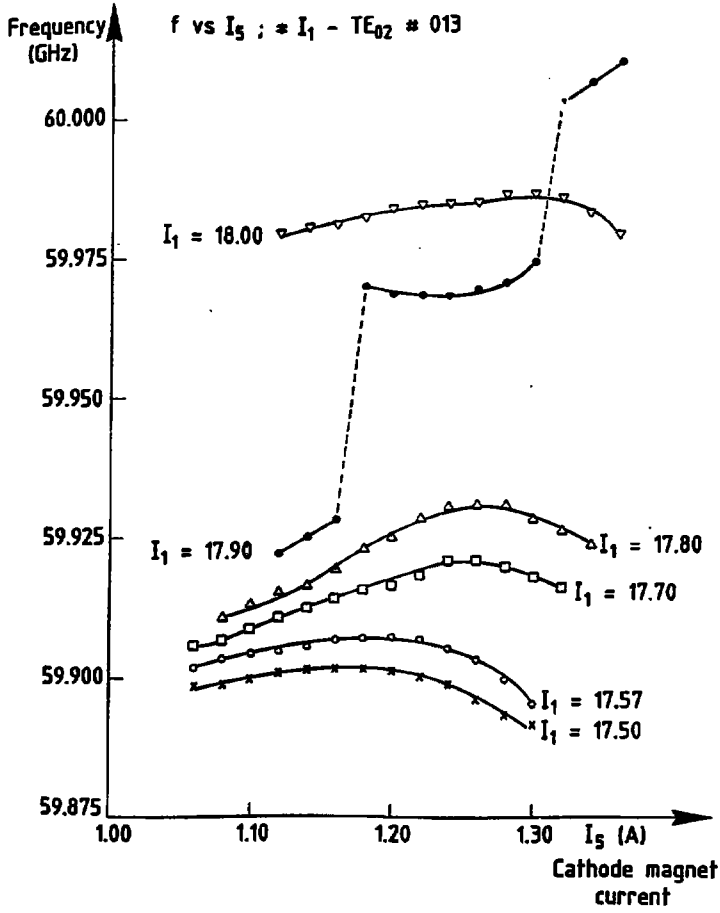
Frequency (GHz)
f vs I_5 ; * I_1 - TE_{02} * 013
60.000
59.975
59.950
59.925
59.900
59.875
I_1 = 18.00
I_1 = 17.90
I_1 = 17.80
I_1 = 17.70
I_1 = 17.57
I_1 = 17.50
1.00
1.10
1.20
1.30
I_5 (A)
Cathode magnet current

Fig. 30

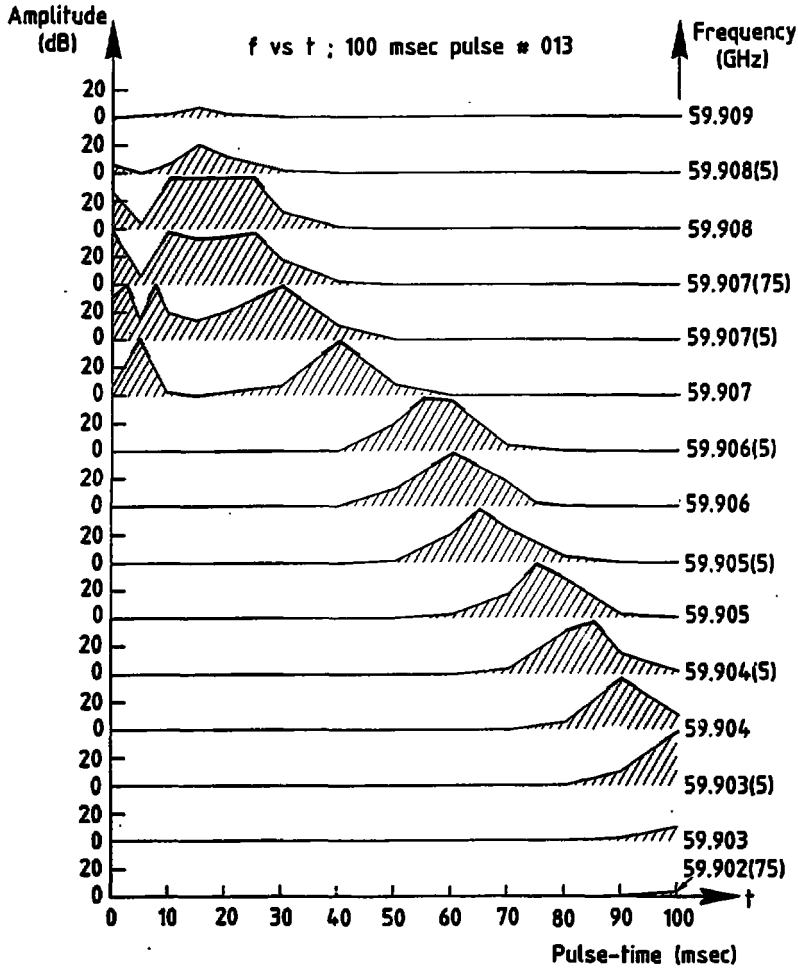
Amplitude
(dB)
f vs t ; 100 msec pulse # 013
Frequency
(GHz)
20
0
59.909
59.908(5)
59.908
59.907(75)
59.907(5)
59.907
59.906(5)
59.906
59.905(5)
59.905
59.904(5)
59.904
59.903(5)
59.903
59.902(75)
t
0
10
20
30
40
50
60
70
80
90
100
Pulse-time (msec)

Fig. 31

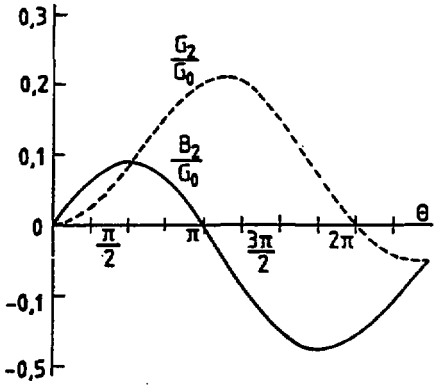

Fig. 32

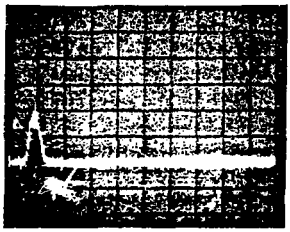

a f = 59.920 GHz

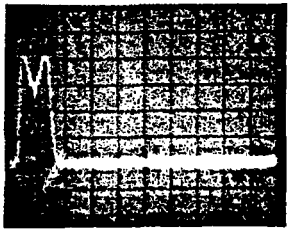

b f = 59.919(5) GHz

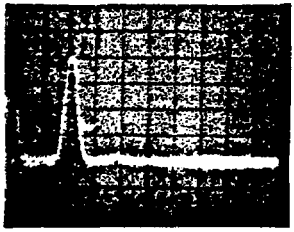

c f = 59.919 GHz

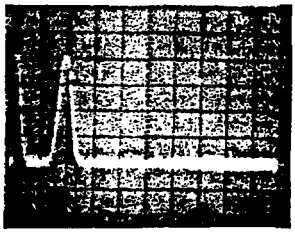

d f = 59.918(5) GHz

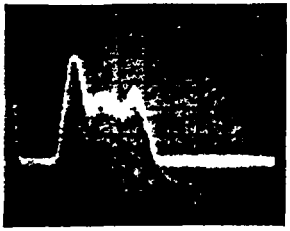

e f = 59.918(25) GHz

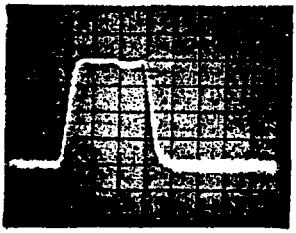

f f = 59.918 GHz

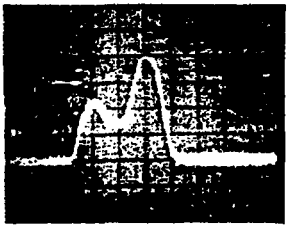

g f = 59.917(75) GHz

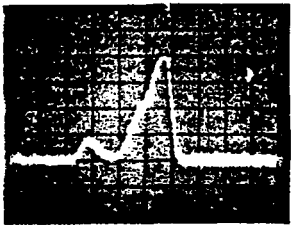

h f = 59.917(5) GHz

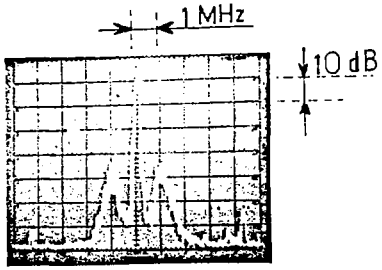

Fig 33

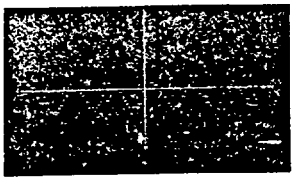

Fig 34 a

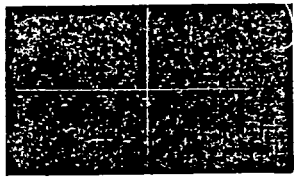

Fig 34 b

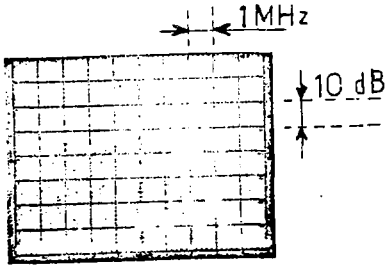

Fig 35